

Practical Distributed Control for VTOL UAVs to Pass a Virtual Tube

Quan Quan, Rao Fu, Mengxin Li, Donghui Wei, Yan Gao and Kai-Yuan Cai

Abstract—Unmanned Aerial Vehicles (UAVs) are now becoming increasingly accessible to amateur and commercial users alike. An air traffic management (ATM) system is needed to help ensure that this newest entrant into the skies does not collide with others. In an ATM, airspace can be composed of *airways*, *intersections* and *nodes*. In this paper, for simplicity, distributed coordinating the motions of Vertical TakeOff and Landing (VTOL) UAVs to pass an *airway* is focused. This is formulated as a *virtual tube passing problem*, which includes passing a virtual tube, inter-agent collision avoidance and keeping within the virtual tube. Lyapunov-like functions are designed elaborately, and formal analysis based on *invariant set theorem* is made to show that all UAVs can pass the virtual tube without getting trapped, avoid collision and keep within the virtual tube. What is more, by the proposed distributed control, a VTOL UAV can keep away from another VTOL UAV or return back to the virtual tube as soon as possible, once it enters into the safety area of another or has a collision with the virtual tube during it is passing the virtual tube. Simulations and experiments are carried out to show the effectiveness of the proposed method and the comparison with other methods.

Index Terms—Distributed control, swarm, UAVs, air traffic, virtual tube.

I. INTRODUCTION

Airspace is utilized today by far lesser aircraft than it can accommodate, especially low altitude airspace. There are more and more applications for UAVs in low altitude airspace, ranging from the on-demand package delivery to traffic and wildlife surveillance, inspection of infrastructure, search and rescue, agriculture, and cinematography. Moreover, since UAVs are usually small owing to portability requirements, it is often necessary to deploy a team of UAVs to accomplish certain missions. All these applications share a common need for both navigation and airspace management. One good starting point is NASA's Unmanned Aerial System Traffic Management (UTM) project, which organized a symposium to begin preparations of a solution for low altitude traffic management to be proposed to the Federal Aviation Administration. What is more, air traffic for UAVs is attracted more and more research [1],[2]. Traditionally, the main role of air traffic management (ATM) is to keep a prescribed separation among all aircraft by using centralized control. However, it is infeasible for increasing UAVs because the traditional control method lacks scalability. In order to

address such a problem, free flight is a developing air traffic control method that uses no centralized control. Instead, parts of airspace are reserved dynamically and automatically in a distributed way using computer communication to ensure the required separation among aircraft. This new system may be implemented into the U.S. air traffic control system in the next decade. Airspace may be allocated temporarily by an ATM for a special task within a given time interval. In this airspace, these aircraft have to be managed so that they can complete their tasks meanwhile avoiding collision. In [1], the airspace is structured similarly to the road network as shown in Figure 1(a). Aircraft are only allowed inside the following three: *airways* playing a similar role to roads or virtual tubes, *intersections* formed by at least two airways, and *nodes* which are the points of interest reachable through an alternating sequence of airways and intersections.

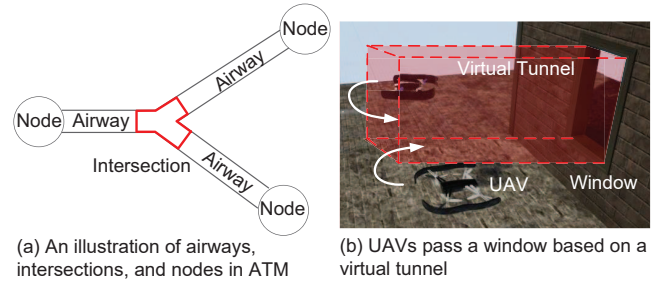


Fig. 1. Practical application scenarios of virtual tube passing problem.

In this paper, for simplicity, coordinating the motions of VTOL UAVs to pass an *airway* is considered, which can be taken as a virtual tube or corridor in the air. Concretely, the main problem is to coordinate the motions of VTOL UAVs include passing a virtual tube, inter-agent conflict (coming within the minimum allowed distance between each other, not to be confused with a *collision*) avoidance and keeping within the virtual tube, which is called the *virtual tube passing problem* here, which is very common in practice. For example, virtual tubes can be paths connecting two places, designed to bypass areas having the dense population or to be covered by wireless mobile networks (4G or 5G). virtual tubes can also be gates, corridors or windows, because they can be viewed as virtual virtual tubes, as shown in Figure 1(b). Such problems of coordination of multiple agents have been addressed partly using different approaches, various stability criteria and numerous control techniques [3],[4],[5],[6],[7],[8],[9]. A commonly-used method, namely the dynamic region-following formation control, is to organize multiple agents as a group

Q. Quan, R. Fu, M. Li, Y. Gao and K-Y. Cai are with the School of Automation Science and Electrical Engineering, Beihang University, Beijing 100191, China (e-mail: qq_buaa@buaa.edu.cn; buaafurao@buaa.edu.cn; lmxin@buaa.edu.cn; buaa_gaoyan@buaa.edu.cn; kycai@buaa.edu.cn).

D. Wei is with the Beijing Electro-Mechanical Engineering Institute, Beijing 100074, China (e-mail: weidonghui2652@sina.com).

inside a region and then move the group to pass virtual tubes, where the size of the region can vary according to the virtual tubes [10],[11],[12],[13]. However, the formation control is not very suited for the air traffic control problem considered. First, each UAV has its own task, while the formation control means that one has to wait for other ones. Second, higher-level coordination should be made to decide which ones should be in one group. What is more, the number of UAVs in airspace is varying dynamically, which increases the design difficulty of the higher-level coordination. Another way is to plan the trajectories for UAVs [14],[15],[16]. However, planning often depends on global information and may have to be updated due to uncertainties in practice, which brings more complex calculations.

According to the consideration above, we propose distributed control for VTOL UAV swarm, each one having the same control protocol. Distributed control will not use the global information so that the computation only depends on the number of local UAVs [17],[18],[19],[20]. This framework is applicable to dense air traffic. By the proposed protocol, every UAV can pass a virtual tube freely not in formation, meanwhile avoiding conflict with each other and keeping within the virtual tube once it enters into the virtual tube. During the process, some UAVs with high speed will overtake slow ones. The idea used is similar to artificial potential field methods because of its ease-of-use, where designed barrier functions [21] are taken as artificial potential functions. The distributed control laws use the negative gradient of mixing of attractive and repulsive potential functions to produce vector fields that ensure the passing and conflict avoidance, respectively. However, it is not easy to use such an idea, with two reasons in the following.

- The guidance strategy for each UAV has to design. An easy method is to set a chain of waypoints for each UAV. However, UAVs may get trapped when using this method. Namely, they have not arrived at their corresponding waypoints, but velocities are zero. Consequently, in order to avoid trap, a higher-level decision should be made to set these waypoints. As indicated by [22], the complexity of the calculation of undesired equilibria remains an open problem. An example is proposed in [16], modelling the virtual tube passing problem as an objective optimization problem, which can get the optimal path to minimize the length, time or energy by designing suitable optimization-based algorithm and objective functions. This algorithm works well for offline path-planning. However, if the obstacles to avoid are dynamic, the optimization-based algorithm will consume a lot of time to update global information and the corresponding constraints during the online path-planning process, which is not suitable for dense air traffic because of lacking real-time of control. Compared to the optimal solution of targets, safety, real-time and reliability are more necessary in practice.
- Besides this problem, the second problem is also encountered in practice especially for UAVs outdoor. The conflict of two agents is often defined in control strategies that their distance is less than a safety distance. The area is called *safety area* of an agent if the distance to the agent

is less than the safety distance. However, a conflict will happen in practice even if conflict avoidance is proved formally because some assumptions will be violated in practice. For example, a UAV may enter into the safety area of another due to an unpredictable communication delay. On the other hand, most likely, two UAVs may not have a real collision in physics because the safety distance is often set large by considering various uncertainties, such as estimate error, communication delay, and control delay. This is a big difference from some indoor robots with a highly accurate position estimation and control. In most literature, if their distance is less than a safety distance, then their control schemes either do not work or even push the agent towards the center of the safety area rather than leaving the safety area. For example, some studies have used the following barrier function terms for collision avoidance, such as $1/\left(\|\mathbf{p}_i - \mathbf{p}_j\|^2 - R\right)$ [23, p. 323] or $\ln(\|\mathbf{p}_i - \mathbf{p}_j\| - R)$ [24], where $\mathbf{p}_i, \mathbf{p}_j$ are two UAVs' positions, and $R > 0$ is the separation distance. The principle is to design a controller to make the barrier function terms bounded so that $\|\mathbf{p}_i - \mathbf{p}_j\|^2 > R$ if $\|\mathbf{p}_i(0) - \mathbf{p}_j(0)\|^2 > R$. Otherwise, $\|\mathbf{p}_i - \mathbf{p}_j\|^2 = R$ will make the barrier function term unbounded. The separation distance for robots indoor is often the sum of the two robots' physical radius, namely $\|\mathbf{p}_i - \mathbf{p}_j\|^2 < R$ will not happen in practice. But, the separation distance is set largely for UAVs compared with their sizes. Due to some uncertainties such as communication delay, $\|\mathbf{p}_i - \mathbf{p}_j\|^2 < R$ will happen in the air. As a consequence, the control corresponding to the barrier function terms mentioned above will make $\|\mathbf{p}_i - \mathbf{p}_j\|^2 \rightarrow 0$ if $1/\left(\|\mathbf{p}_i - \mathbf{p}_j\|^2 - R\right)$ is used (the two UAVs are pushed together by the design controller) or appear numerical computation error if $\ln(\|\mathbf{p}_i - \mathbf{p}_j\| - R)$ is used.

Motivated by these problems, practical distributed control is proposed here to solve the virtual tube passing problem. Such a problem can be classified into a *basic virtual tube passing problem* and a *general virtual tube passing problem*. The former only considers that all UAVs are within the virtual tube at the beginning, while the latter allows UAVs at everywhere in the beginning. For the basic virtual tube passing problem, in light of artificial potential field methods, one Lyapunov function and two barrier functions are designed elaborately for approaching the finishing line, avoiding conflict with other UAVs, and keeping within the virtual tube, respectively. The distributed controller design is based on the combination of the three Lyapunov-like functions. A formal proof is given to show that all UAVs can pass the virtual tube without trapping, avoid conflict and keep within the virtual tube. What is more, by the proposed control, a UAV can keep away from another UAV or return back to the virtual tube as soon as possible, once it enters into the safety area of another UAV or has a conflict with the virtual tube during it is passing the virtual tube. For the general virtual tube passing problem, several virtual tube type areas are defined to cover the whole airspace. As a consequence, the general virtual tube passing problem is decomposed into several basic virtual tube passing problems.

As a result, for UAVs in different areas, they have different controllers according to the design of the basic virtual tube passing problem. By switching these controllers, the general virtual tube passing problem can be solved.

The practicability of the proposed distributed control lies on the following six features:

- *No ID required.* Unlike the formation control, neighboring UAVs' IDs of a UAV are not required by the proposed distributed control. Some active detection devices such as cameras or radars may only detect neighboring UAVs' position and velocity but no IDs, because these UAVs may look similarly. This implies that the proposed distributed control can work autonomously without communication.
- *Practical model used.* A double integral model with the given velocity command as input is proposed for UAVs. This model is simple and easy to obtain. What is more, distributed control is developed for various tasks based on commercial semi-autonomous autopilots.
- *Control saturation.* The maximum velocity command in the proposed distributed controller is confined according to the requirement of semi-autonomous autopilots.
- *Conflict-free.* A formal proof about conflict avoidance and keeping within the virtual tube is given. Even if a UAV enters into the safety area of another UAV or has a conflict with the virtual tube, it can keep away from the UAV or can return back to the virtual tube as soon as possible.
- *Convergence.* A formal proof is given to show that all UAVs pass the finishing line without getting trapped.
- *Low time complexity.* The proposed control protocol is simple and can be computed at high speed, which is more suitable for dense air traffic than optimization-based algorithms. The calculation time of finding feasible solutions for different strategies will be compared in simulation.

The paper is organised as follows. In Section II, a UAV control model is proposed, which contains the filtered position model and three types of areas, to formulate the virtual tube passing problem composed of a basic one and a general one. Some functions for different purposes are introduced in Section III for controller design. In Section IV, a controller is designed based on Lyapunov-like functions to solve the basic virtual tube passing problem, where the stability analysis is made. In Section V, a controller is designed based on Lyapunov-like functions to solve the general virtual tube passing problem, by decomposing this problem into several basic virtual tube passing problems. The effectiveness of the proposed method is demonstrated by simulation and flight experiments in Section VI. The conclusions are given in Section VII. Some details of mathematical proof process are given in Section VIII as appendix.

II. PROBLEM FORMULATION

In this section, a UAV control model is introduced first, including three types of areas, namely safety area, avoidance area, and detection area, used for control. Then, the virtual tube passing problem is formulated into a basic one and a general one depending on the initial places of UAVs.

A. UAV Control Model

1) *Position Model:* There are M VTOL UAVs in local airspace at the same altitude satisfying the following model

$$\begin{aligned}\dot{\mathbf{p}}_i &= \mathbf{v}_i \\ \dot{\mathbf{v}}_i &= -l_i (\mathbf{v}_i - \mathbf{v}_{c,i})\end{aligned}\quad (1)$$

where $l_i > 0$, $\mathbf{p}_i \in \mathbb{R}^2$ and $\mathbf{v}_i \in \mathbb{R}^2$ are the position and velocity of the i th VTOL UAV, $\mathbf{v}_{c,i} \in \mathbb{R}^2$ is the velocity command of the i th UAV, $i = 1, 2, \dots, M$. The control gain l_i depends on the i th UAV and the semi-autonomous autopilot used, which can be obtained through flight experiments. From the model (1), $\lim_{t \rightarrow \infty} \|\mathbf{v}_i(t) - \mathbf{v}_{c,i}\| = 0$ if $\mathbf{v}_{c,i}$ is constant. Here, the velocity command $\mathbf{v}_{c,i}$ for the i th VTOL UAV, is subject to a saturation defined as where $v_{m,i} > 0$ is the maximum speed of the i th VTOL UAVs, $i = 1, 2, \dots, M$, $\mathbf{v} \triangleq [v_1 \ v_2]^T \in \mathbb{R}^2$. The saturation function $\text{sat}(\mathbf{v}, v_{m,i})$ and the vector \mathbf{v} are parallel all the time so it can keep the flying direction the same if $\|\mathbf{v}\| > v_{m,i}$ [23]. The saturation function can be rewritten as

$$\text{sat}(\mathbf{v}, v_{m,i}) = \kappa_{v_{m,i}}(\mathbf{v}) \mathbf{v} \quad (2)$$

where

$$\kappa_{v_{m,i}}(\mathbf{v}) \triangleq \begin{cases} 1, & \|\mathbf{v}\| \leq v_{m,i} \\ \frac{v_{m,i}}{\|\mathbf{v}\|}, & \|\mathbf{v}\| > v_{m,i} \end{cases}.$$

It is obvious that $0 < \kappa_{v_{m,i}}(\mathbf{v}) \leq 1$. Sometimes, $\kappa_{v_{m,i}}(\mathbf{v})$ will be written as $\kappa_{v_{m,i}}$ for short. According to this, if and only if $\mathbf{v} = \mathbf{0}$, then

$$\mathbf{v}^T \text{sat}(\mathbf{v}, v_{m,i}) = 0. \quad (3)$$

Remark 1. It is well-known that a typical multicopter is a physical system with underactuated dynamics [23, pp.126-130]. But, many organizations or companies have designed some open source semi-autonomous autopilots or offered semi-autonomous autopilots with software development kits. The semi-autonomous autopilots can be used for velocity control of VTOL UAVs. For example, A3 autopilots released by DJI allow the range of the horizontal velocity command from $-10\text{m/s} \sim 10\text{m/s}$ [25]. With such an autopilot, the velocity of a VTOL UAV can track a given velocity command in a reasonable time. Not only can this avoid the trouble of modifying the low-level source code of autopilots, but also it can utilize commercial autopilots to complete various tasks. So, the dynamics (1) is practical especially for higher-level control.

2) *Filtered Position Model:* In this section, the motion of each VTOL UAV is transformed into a single integrator form to simplify the controller design and analysis. As shown in Figure 2, although the position distances of the three cases are the same, namely a marginal avoidance distance, the case in Figure 2(b) needs to carry out avoidance urgently by considering the velocity. However, the case in Figure 2(a) in fact does not need to be considered to perform collision avoidance. With such an intuition, a filtered position is defined as follows:

$$\boldsymbol{\xi}_i \triangleq \mathbf{p}_i + \frac{1}{l_i} \mathbf{v}_i. \quad (4)$$

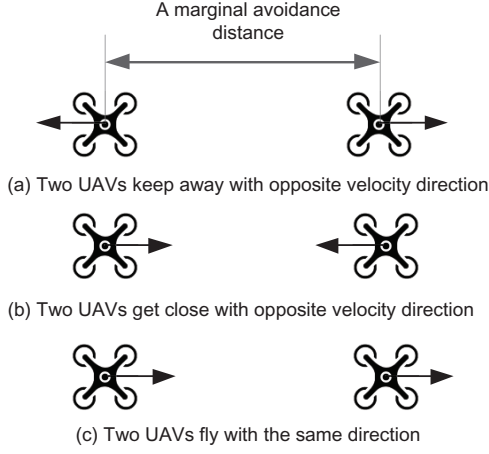


Fig. 2. Intuitive interpretation for filtered position

Then

$$\begin{aligned}\dot{\xi}_i &= \dot{\mathbf{p}}_i + \frac{1}{l_i} \dot{\mathbf{v}}_i \\ &= \mathbf{v}_i - \frac{1}{l_i} l_i (\mathbf{v}_i - \mathbf{v}_{c,i}) \\ &= \mathbf{v}_{c,i}\end{aligned}\quad (5)$$

where $i = 1, 2, \dots, M$. Let

$$r_v = \max_i \frac{v_{m,i}}{l_i}. \quad (6)$$

In the following, a relationship between the position error and the filtered position error is shown.

Proposition 1. Given any $r > 0$, for the i th and j th VTOL UAVs, if $\|\mathbf{v}_i(0)\| \leq v_{m,i}$ and the filtered position error satisfies $\|\xi_i(t) - \xi_j(t)\| \geq r + 2r_v$, then

$$\|\mathbf{p}_i(t) - \mathbf{p}_j(t)\| \geq r$$

$t \geq 0$, where $i, j = 1, 2, \dots, M$, $i \neq j$, $r > 0$.

Proof. See Appendix. \square

B. Three Types of Areas around a UAV

In light of [17], three types of areas used for control, namely safety area, avoidance area, and detection area, are defined. Unlike [17], these areas are suit for UAVs and the velocity is further introduced.

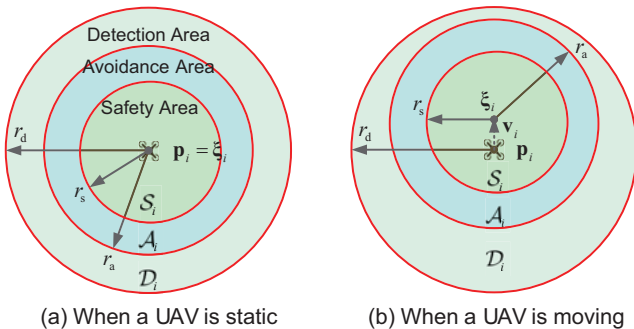


Fig. 3. Safety area, avoidance area and detection area of a UAV.

1) *Safety Area:* In order to avoid a conflict, as shown in Figure 3, the *safety radius* r_s of a UAV is defined as

$$\mathcal{S}_i = \{\mathbf{x} \in \mathbb{R}^2 \mid \|\mathbf{x} - \xi_i\| \leq r_s\} \quad (7)$$

where $r_s > 0$ is the safety radius, $i = 1, 2, \dots, M$. It should be noted that we consider the velocity of the i th UAV in the definition of \mathcal{S}_i . For all UAVs, no *confliction* with each other implies

$$\mathcal{S}_i \cap \mathcal{S}_j = \emptyset$$

namely

$$\|\xi_j - \xi_i\| > 2r_s. \quad (8)$$

Proposition 1 implies that two VTOL UAVs will be separated largely enough if (8) is satisfied with a safety radius r_s large enough.

2) *Avoidance Area:* Besides the safety area, there exists an *avoidance area* used for starting avoidance control. If another UAV is out of the avoidance area of the i th UAV, then the object will not need to be avoided. For the i th UAV, the *avoidance area* for other UAVs is defined as

$$\mathcal{A}_i = \{\mathbf{x} \in \mathbb{R}^2 \mid \|\mathbf{x} - \xi_i\| \leq r_a\} \quad (9)$$

where $r_a > 0$ is the *avoidance radius*, $i = 1, 2, \dots, M$. It should be noted that we consider the velocity of the i th UAV in the definition of \mathcal{A}_i . If

$$\mathcal{A}_i \cap \mathcal{S}_j \neq \emptyset,$$

namely

$$\|\xi_i - \xi_j\| \leq r_a + r_s$$

then the j th UAV should be avoided by the i th UAV. Since

$$\mathcal{A}_i \cap \mathcal{S}_j \neq \emptyset \Leftrightarrow \mathcal{A}_j \cap \mathcal{S}_i \neq \emptyset$$

according to the definition of \mathcal{A}_i , the i th UAV should be avoided by the j th UAV at the same time. When the j th UAV just enters into the avoidance area of the i th UAV, it is required that they have not conflicted at the beginning. Therefore, we require

$$r_a > r_s.$$

3) *Detection Area:* By cameras, radars, or Vehicle to Vehicle (V2V) communication, the UAVs can receive the positions and velocities of their neighboring UAVs. The *detection area* only depends on the detection range of the used devices, which is only related to its position. For the i th UAV, this area is defined as

$$\mathcal{D}_i = \{\mathbf{x} \in \mathbb{R}^2 \mid \|\mathbf{x} - \mathbf{p}_i\| \leq r_d\} \quad (10)$$

where $r_d > 0$ is the *detection radius*, $i = 1, 2, \dots, M$. When another UAV is within this area, it can be detected.

Proposition 2. Suppose $r_d > r_s + r_a + 2r_v$, $i = 1, 2, \dots, M$. Then for any $i \neq j$, if $\mathcal{A}_i \cap \mathcal{S}_j \neq \emptyset$, then $\mathbf{p}_j \in \mathcal{D}_i$, $i, j = 1, 2, \dots, M$.

Proof. It is similar to proof of *Proposition 1*. \square

To simplify the following problems, we have the following assumption for all VTOL UAVs.

Assumption 1. The radius of the detection area satisfies $r_d > r_s + r_a + 2r_v$.

According to *Assumption 1*, for the i th UAV, any other UAV entering into its avoidance area can be detected by the i th UAV and will not conflict with the i th UAV initially, $i = 1, 2, \dots, M$.

C. virtual tube Passing Problem Formulation

In a horizontal plane, as shown in Figure 4, a virtual tube (analogous to an *airway* or a *highway* on the ground) here is a horizontal long band with the width $2r_t$ and centerline starting from $\mathbf{p}_{t,1} \in \mathbb{R}^2$ to $\mathbf{p}_{t,2} \in \mathbb{R}^2$, where $r_t > Lr_a$, where $L \in \mathbb{Z}_+$ is the lane number in the virtual tube allowed for UAVs.

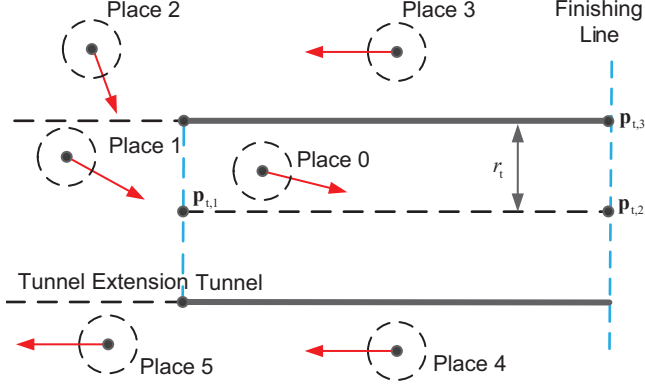


Fig. 4. Airspace and virtual tube.

Define

$$\begin{aligned} \mathbf{A}_{t,12}(\mathbf{p}_{t,1}, \mathbf{p}_{t,2}) &\triangleq \mathbf{I}_2 - \frac{(\mathbf{p}_{t,1} - \mathbf{p}_{t,2})(\mathbf{p}_{t,1} - \mathbf{p}_{t,2})^T}{\|\mathbf{p}_{t,1} - \mathbf{p}_{t,2}\|^2} \\ \mathbf{A}_{t,23}(\mathbf{p}_{t,2}, \mathbf{p}_{t,3}) &\triangleq \mathbf{I}_2 - \frac{(\mathbf{p}_{t,2} - \mathbf{p}_{t,3})(\mathbf{p}_{t,2} - \mathbf{p}_{t,3})^T}{\|\mathbf{p}_{t,2} - \mathbf{p}_{t,3}\|^2}. \end{aligned} \quad (11)$$

Here, matrix $\mathbf{A}_{t,12} = \mathbf{A}_{t,12}^T$, $\mathbf{A}_{t,23} = \mathbf{A}_{t,23}^T \in \mathbb{R}^{2 \times 2}$ are positive semi-definite matrices. According to the projection operator [26, p. 480], the value $\|\mathbf{A}_{t,12}(\mathbf{p} - \mathbf{p}_{t,1})\|$ is the distance from $\mathbf{p} \in \mathbb{R}^2$ to the straight line $\overline{\mathbf{p}_{t,1}\mathbf{p}_{t,2}}$ as shown in Figure 5. Particularly, the equation $\|\mathbf{A}_{t,12}(\mathbf{p} - \mathbf{p}_{t,1})\| = 0$ implies that \mathbf{p} is on the straight-line $\overline{\mathbf{p}_{t,1}\mathbf{p}_{t,2}}$. Similarly, the value $\|\mathbf{A}_{t,23}(\mathbf{p} - \mathbf{p}_{t,2})\|$ is the distance from \mathbf{p} to the finishing line $\overline{\mathbf{p}_{t,2}\mathbf{p}_{t,3}}$. Define position errors as

$$\begin{aligned} \tilde{\mathbf{p}}_{1,i} &\triangleq \mathbf{A}_{t,23}(\mathbf{p}_i - \mathbf{p}_{t,2}) \\ \tilde{\mathbf{p}}_{m,ij} &\triangleq \mathbf{p}_i - \mathbf{p}_j \\ \tilde{\mathbf{p}}_{t,i} &\triangleq \mathbf{A}_{t,12}(\mathbf{p}_i - \mathbf{p}_{t,1}) \end{aligned}$$

and the filtered position errors as

$$\begin{aligned} \tilde{\xi}_{1,i} &\triangleq \mathbf{A}_{t,23}(\xi_i - \mathbf{p}_{t,2}) \\ \tilde{\xi}_{m,ij} &\triangleq \xi_i - \xi_j \\ \tilde{\xi}_{t,i} &\triangleq \mathbf{A}_{t,12}(\xi_i - \mathbf{p}_{t,1}) \end{aligned}$$

where $i, j = 1, 2, \dots, M$. With the definitions above, according to (1), the derivatives of the filtered errors are

$$\dot{\tilde{\xi}}_{1,i} = \mathbf{A}_{t,23}\mathbf{v}_{c,i} \quad (12)$$

$$\dot{\tilde{\xi}}_{m,ij} = \mathbf{v}_{c,i} - \mathbf{v}_{c,j} \quad (13)$$

$$\dot{\tilde{\xi}}_{t,i} = \mathbf{A}_{t,12}\mathbf{v}_{c,i} \quad (14)$$

where $i, j = 1, 2, \dots, M$.

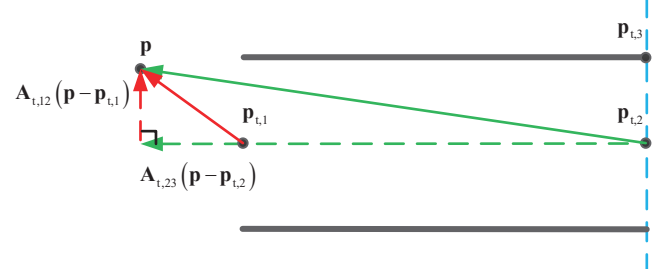


Fig. 5. Diagram of the projective operator.

With the description above, the following assumptions are proposed.

Assumption 2. As shown in Figure 4, the initial condition $\mathbf{p}_i(0), \xi_i(0)$, $i = 1, 2, \dots, M$ are all within the virtual tube or its extension, namely

$$\begin{aligned} \left(\frac{\mathbf{p}_{t,2} - \mathbf{p}_{t,1}}{\|\mathbf{p}_{t,2} - \mathbf{p}_{t,1}\|} \right)^T (\mathbf{p}_i(0) - \mathbf{p}_{t,2}) &< 0 \\ \left(\frac{\mathbf{p}_{t,2} - \mathbf{p}_{t,1}}{\|\mathbf{p}_{t,2} - \mathbf{p}_{t,1}\|} \right)^T (\xi_i(0) - \mathbf{p}_{t,2}) &< 0 \end{aligned}$$

where $\overline{\mathbf{p}_{t,2}\mathbf{p}_{t,3}}$ is perpendicular to $\overline{\mathbf{p}_{t,1}\mathbf{p}_{t,2}}$ with $\|\mathbf{p}_{t,2} - \mathbf{p}_{t,1}\| = r_t$.

Assumption 2'. As shown in Figure 4, the initial condition $\xi_i(0)$ are not all within the virtual tube or its extension, but locate the left of the finishing line $\overline{\mathbf{p}_{t,2}\mathbf{p}_{t,3}}$.

Assumption 3. The UAVs' initial conditions satisfy

$$\|\xi_i(0) - \xi_j(0)\| > 2r_s, i \neq j$$

and $\|\mathbf{v}_i(0)\| \leq v_m$, where $i, j = 1, 2, \dots, M$.

Assumption 4. Once a UAV arrives near the finishing line $\overline{\mathbf{p}_{t,2}\mathbf{p}_{t,3}}$, then it will quit the virtual tube not to affect the UAVs behind. Mathematically, given $\epsilon_0 \in \mathbb{R}_+$, a UAV arrives near the finishing line $\overline{\mathbf{p}_{t,2}\mathbf{p}_{t,3}}$ if

$$(\mathbf{p}_{t,2} - \mathbf{p}_{t,1})^T \mathbf{A}_{t,23}(\mathbf{p}_i - \mathbf{p}_{t,2}) \geq -\epsilon_0. \quad (15)$$

Neighboring Set. Let the set $\mathcal{N}_{m,i}$ be the collection of all mark numbers of other VTOL UAVs whose safety areas enter into the avoidance area of the i th UAV, namely

$$\mathcal{N}_{m,i} = \{j | \mathcal{S}_j \cap \mathcal{A}_i \neq \emptyset, j = 1, \dots, M, i \neq j\}.$$

For example, if the safety areas of the 1th, 2th VTOL UAVs enter into in the avoidance area of the 3th UAV, then $\mathcal{N}_{m,3} = \{1, 2\}$. Based on *Assumptions* and *definition* above, two types of *virtual tube passing problems* are stated in the following.

- **Basic virtual tube passing problem.** Under *Assumptions 1-4*, design the velocity input $\mathbf{v}_{c,i}$ for the i th UAV with local information from $\mathcal{N}_{m,i}$ to guide it to fly to pass the virtual tube until it arrives near the finishing line $\overline{\mathbf{p}_{t,2}\mathbf{p}_{t,3}}$, meanwhile avoiding colliding other UAVs ($\|\tilde{\xi}_{m,ij}\| > 2r_s$) and keeping within the virtual tube ($\|\tilde{\xi}_{t,i}\| < r_t - r_s$) while passing it, $i = 1, 2, \dots, M$.
- **General virtual tube passing problem.** Under *Assumptions 1,2',3,4*, design the velocity input $\mathbf{v}_{c,i}$ for the i th

UAV with local information from $\mathcal{N}_{m,i}$ to guide it to fly to pass the virtual tube until it arrives near the finishing line $\overline{\mathbf{p}_{t,2}\mathbf{p}_{t,3}}$, meanwhile avoiding conflict with other UAVs ($\|\tilde{\xi}_{m,ij}\| > 2r_s$) and keeping within the virtual tube when passing it ($\|\tilde{\xi}_{t,i}\| < r_t - r_s$), $i = 1, 2, \dots, M$.

Remark 1. As shown in Figure 6, if $(\mathbf{p}_{t,2} - \mathbf{p}_{t,1})^T (\mathbf{p}_i - \mathbf{p}_{t,2}) > 0$, then \mathbf{p}_i locates the right side of the finishing line $\overline{\mathbf{p}_{t,2}\mathbf{p}_{t,3}}$; if $(\mathbf{p}_{t,2} - \mathbf{p}_{t,1})^T (\mathbf{p}_i - \mathbf{p}_{t,2}) < 0$, then \mathbf{p}_i locates the left side of the finishing line $\overline{\mathbf{p}_{t,2}\mathbf{p}_{t,3}}$.

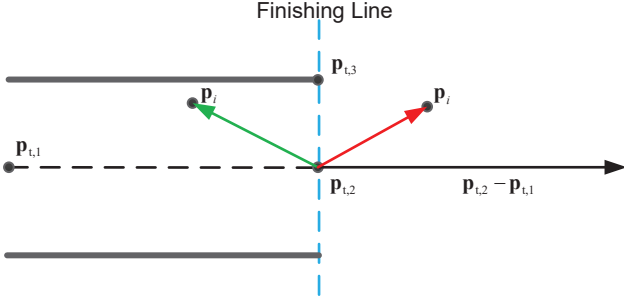


Fig. 6. Position relative to the finishing line.

Remark 2. For Assumption 2, all UAVs are within the virtual tube (like Place 0 in Figure 4) or its extension (like Place 1 in Figure 4). For Assumption 2', UAVs are not all within the virtual tube or its extension. This implies that UAVs may locate everywhere. For example, UAVs may locate the places, like Place 0, ..., Place 5 shown in Figure 4.

III. PRELIMINARIES

A. Line Integral Lyapunov Function

In the following, we will design a new type of Lyapunov functions, called *Line Integral Lyapunov Function*. This type of Lyapunov functions is inspired by its scalar form [27, p.74]. If $xf(x) > 0$ for $x \neq 0$, then $V_{li}'(y) = \int_0^y f(x)dx > 0$ when $y \neq 0$. The derivative is $\dot{V}_{li}' = f(y)\dot{y}$. A line integral Lyapunov function for vectors is defined as

$$V_{li}(\mathbf{y}) = \int_{C_y} \text{sat}(\mathbf{x}, a)^T d\mathbf{x} \quad (16)$$

where $a > 0$, $\mathbf{x} \in \mathbb{R}^n$, C_y is a line from $\mathbf{0}$ to $\mathbf{y} \in \mathbb{R}^n$. In the following lemma, we will show its properties.

Lemma 1. Suppose that the line integral Lyapunov function V_{li} is defined as (16). Then (i) $V_{li}(\mathbf{y}) > 0$ if $\|\mathbf{y}\| \neq 0$; (ii) if $\|\mathbf{y}\| \rightarrow \infty$, then $V_{li}(\mathbf{y}) \rightarrow \infty$; (iii) if $V_{li}(\mathbf{y})$ is bounded, then $\|\mathbf{y}\|$ is bounded.

Proof. Since

$$\text{sat}(\mathbf{x}, a) = \kappa_a(\mathbf{x}) \mathbf{x}$$

the function (16) can be written as

$$V_{li}(\mathbf{y}) = \int_{C_y} \kappa_a(\mathbf{x}) \mathbf{x}^T d\mathbf{x} \quad (17)$$

where

$$\kappa_a(\mathbf{x}) \triangleq \begin{cases} 1, & \|\mathbf{x}\| \leq a \\ \frac{a}{\|\mathbf{x}\|}, & \|\mathbf{x}\| > a \end{cases}.$$

Let $z = \|\mathbf{x}\|$. Then the function (17) becomes

$$\begin{aligned} V_{li}(\mathbf{y}) &= \int_{C_y} \frac{\kappa_a(\mathbf{x})}{2} dz^2 \\ &= \int_0^{\|\mathbf{y}\|} \kappa_a(\mathbf{x}) z dz. \end{aligned}$$

- If $\|\mathbf{y}\| \leq a$, then $\kappa_a(\mathbf{x}) = 1$. Consequently,

$$V_{li}(\mathbf{y}) = \frac{1}{2} \|\mathbf{y}\|^2. \quad (18)$$

- If $\|\mathbf{y}\| > a$, then

$$\int_0^{\|\mathbf{y}\|} \kappa_a(\mathbf{x}) z dz = \int_0^a z dz + \int_a^{\|\mathbf{y}\|} \frac{a}{\|\mathbf{x}\|} z dz.$$

Since $z = \|\mathbf{x}\|$, we have

$$V_{li}(\mathbf{y}) \geq \frac{1}{2} a^2 + a(\|\mathbf{y}\| - a). \quad (19)$$

Therefore, from the form of (18) and (19), we have (i) $V_{li}(\mathbf{y}) > 0$ if $\|\mathbf{y}\| \neq 0$. (ii) if $\|\mathbf{y}\| \rightarrow \infty$, then $V_{li}(\mathbf{y}) \rightarrow \infty$; (iii) if $V_{li}(\mathbf{y})$ is bounded, then $\|\mathbf{y}\|$ is bounded. \square

B. Two Smooth Functions

Two smooth functions are defined for the following Lyapunov-like function design. As shown in Figure 7 (upper plot), define a second-order differentiable ‘bump’ function as [24]

$$\sigma(x, d_1, d_2) = \begin{cases} 1 & \text{if } x \leq d_1 \\ Ax^3 + Bx^2 + Cx + D & \text{if } d_1 \leq x \leq d_2 \\ 0 & \text{if } d_2 \leq x \end{cases} \quad (20)$$

with $A = -2/(d_1 - d_2)^3$, $B = 3(d_1 + d_2)/(d_1 - d_2)^3$, $C = -6d_1d_2/(d_1 - d_2)^3$ and $D = d_2^2(3d_1 - d_2)/(d_1 - d_2)^3$. The derivative of $\sigma(x, d_1, d_2)$ with respect to x is

$$\frac{\partial \sigma(x, d_1, d_2)}{\partial x} = \begin{cases} 0 & \text{if } x \leq d_1 \\ 3Ax^2 + 2Bx + C & \text{if } d_1 \leq x \leq d_2 \\ 0 & \text{if } d_2 \leq x \end{cases}.$$

Define another smooth function as shown in Figure 7 (lower plot) to approximate a saturation function

$$\bar{s}(x) = \min(x, 1), x \geq 0$$

that

$$s(x, \epsilon_s) = \begin{cases} x & 0 \leq x \leq x_1 \\ (1 - \epsilon_s) + \sqrt{\epsilon_s^2 - (x - x_2)^2} & x_1 \leq x \leq x_2 \\ 1 & x_2 \leq x \end{cases} \quad (21)$$

with $x_2 = 1 + \frac{1}{\tan 67.5^\circ} \epsilon_s$ and $x_1 = x_2 - \sin 45^\circ \epsilon_s$. Since it is required $x_1 \geq 0$, one has $\epsilon_s \leq \frac{\tan 67.5^\circ}{\tan 67.5^\circ \sin 45^\circ - 1}$. For any $\epsilon_s \in [0, \frac{\tan 67.5^\circ}{\tan 67.5^\circ \sin 45^\circ - 1}]$, it is easy to see

$$s(x, \epsilon_s) \leq \bar{s}(x) \quad (22)$$

and

$$\lim_{\epsilon_s \rightarrow 0} \sup_{x \geq 0} |\bar{s}(x) - s(x, \epsilon_s)| = 0. \quad (23)$$

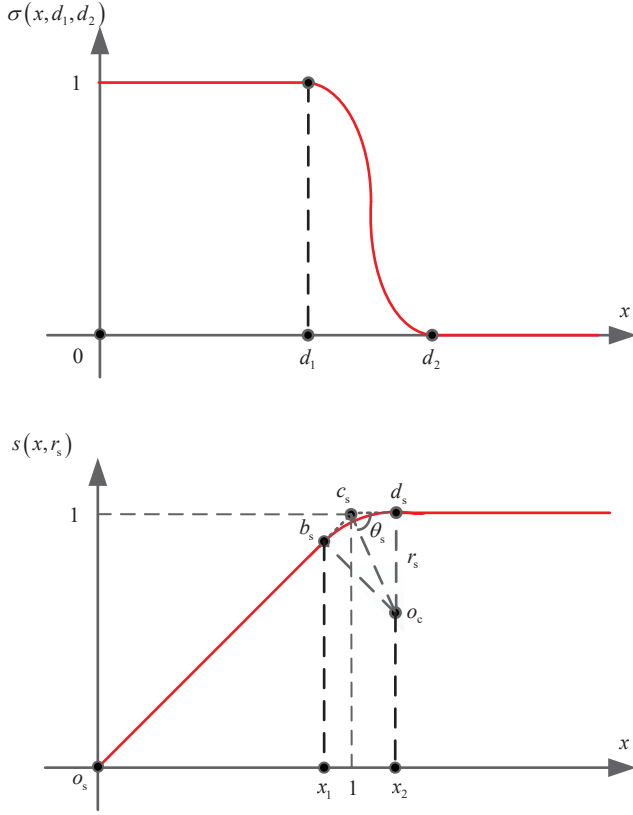


Fig. 7. Two smooth functions. For a smooth saturation function, $\theta_s = 67.5^\circ$.

The derivative of $s(x, \epsilon_s)$ with respect to x is

$$\frac{\partial s(x, \epsilon_s)}{\partial x} = \begin{cases} 1 & 0 \leq x \leq x_1 \\ \frac{x_2 - x}{\sqrt{\epsilon_s^2 - (x - x_2)^2}} & x_1 \leq x \leq x_2 \\ 0 & x_2 \leq x \end{cases}.$$

For any $\epsilon_s > 0$, we have $\sup_{x \geq 0} |\partial s(x, \epsilon_s) / \partial x| \leq 1$.

IV. BASIC VIRTUAL TUBE PASSING PROBLEM

In this section, three Lyapunov-like functions for approaching the finishing line, avoiding conflict, and keeping within the virtual tube are established. Based on them, a controller to solve the basic virtual tube passing problem is derived and then a formal analysis is made.

A. Lyapunov-Like Function Design and Analysis

For the basic virtual tube passing problem, three subproblems are required to solve, namely approaching the finishing line $\overline{\mathbf{p}_{t,2}\mathbf{p}_{t,3}}$, avoiding conflict with other UAVs, and keeping within the virtual tube. Correspondingly, three Lyapunov-like functions are proposed.

1) *Integral Lyapunov Function for Approaching Finishing Line:* Define a smooth curve $C_{\tilde{\xi}_{l,i}}$ from $\mathbf{0}$ to $\tilde{\xi}_{l,i}$. Then, the line integral of $\text{sat}(\mathbf{x}, v_{m,i})$ along $C_{\tilde{\xi}_{l,i}}$ is

$$V_{l,i} = \int_{C_{\tilde{\xi}_{l,i}}} \text{sat}(k_1 \mathbf{x}, v_{m,i})^T d\mathbf{x} \quad (24)$$

where k_1 is an adjustable parameter, $i = 1, 2, \dots, M$. From the definition, $V_{l,i} \geq 0$. According to Thomas' Calculus [28, p. 911], one has

$$V_{l,i} = \int_0^t \text{sat}(k_1 \tilde{\xi}_{l,i}(\tau), v_{m,i})^T \dot{\tilde{\xi}}_{l,i}(\tau) d\tau. \quad (25)$$

The objective of the designed velocity command is to make $V_{l,i}$ be zero. This implies that $\|\tilde{\xi}_{l,i}\|$ goes down to zero according to the property (24), namely the i th UAV approaches the finishing line $\overline{\mathbf{p}_{t,2}\mathbf{p}_{t,3}}$.

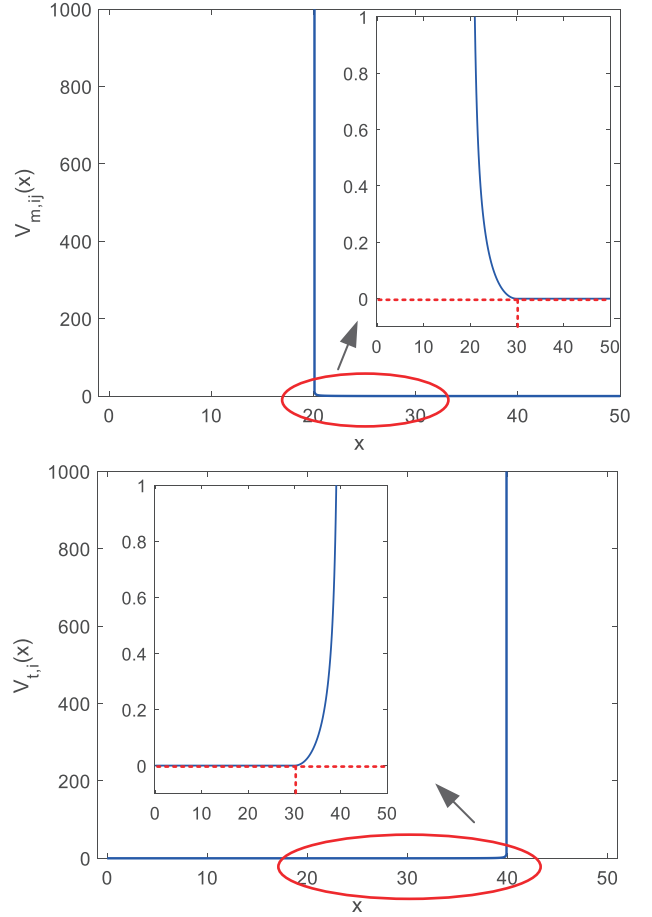


Fig. 8. Barrier functions for avoiding collision and keeping within virtual tube.

2) *Barrier Function for Avoiding Conflict with Other UAVs:* Define

$$V_{m,ij} = \frac{k_2 \sigma_m(\|\tilde{\xi}_{m,ij}\|)}{(1 + \epsilon_m) \|\tilde{\xi}_{m,ij}\| - 2r_s s\left(\frac{\|\tilde{\xi}_{m,ij}\|}{2r_s}, \epsilon_s\right)}. \quad (26)$$

Here $\sigma_m(x) \triangleq \sigma(x, 2r_s, r_a + r_s)$, where $\sigma(\cdot)$ is defined in (20). When $r_s = 10$, $r_a = 20$, $\epsilon_m = 10^{-6}$, $k_2 = 1$, the function $V_{m,ij}$ is shown in Figure 8 (upper plot), where $V_{m,ij}(x) = 0$ as $x \geq r_s + r_a = 30$ and $V_{m,ij}(x)$ is increased sharply as $x \rightarrow 0$ from $x = 30$. The function $V_{m,ij}$ has the following properties:

- Property (i). $\partial V_{m,ij} / \partial \|\tilde{\xi}_{m,ij}\| \leq 0$ as $V_{m,ij}$ is a nonincreasing function with respect to $\|\tilde{\xi}_{m,ij}\|$;

- Property (ii). If $\|\tilde{\xi}_{m,ij}\| > r_a + r_s$, namely $\mathcal{A}_i \cap \mathcal{S}_j = \emptyset$ and $\mathcal{A}_j \cap \mathcal{S}_i = \emptyset$, then $V_{m,ij} = 0$ and $\partial V_{m,ij} / \partial \|\tilde{\xi}_{m,ij}\| = 0$; if $V_{m,ij} = 0$, then $\|\tilde{\xi}_{m,ij}\| > r_a + r_s > 2r_s$;
- Property (iii). If $0 < \|\tilde{\xi}_{m,ij}\| < 2r_s$, namely $\mathcal{S}_j \cap \mathcal{S}_i \neq \emptyset$ (they may not collide in practice), then there exists a sufficiently small $\epsilon_s > 0$ such that

$$V_{m,ij} \approx \frac{k_2}{\epsilon_m \|\tilde{\xi}_{m,ij}\|} \geq \frac{k_2}{2\epsilon_m r_s}. \quad (27)$$

The objective of the designed velocity command is to make $V_{m,ij}$ be zero or as small as possible. According to property (ii), this implies $\|\tilde{\xi}_{m,ij}\| > 2r_s$, namely the i th UAV will not conflict with the j th UAV.

3) *Barrier Function for Keeping within virtual tube*: Define

$$V_{t,i} = \frac{k_3 \sigma_t (r_t - \|\tilde{\xi}_{t,i}\|)}{(r_t - r_s) - \|\tilde{\xi}_{t,i}\| s \left(\frac{r_t - r_s}{\|\tilde{\xi}_{t,i}\| + \epsilon_t}, \epsilon_s \right)}$$

where $\sigma_t(x) \triangleq \sigma(x, r_s, r_a)$. When $r_t = 50$, $r_s = 10$, $r_a = 20$, $\epsilon_t = 10^{-6}$, $k_3 = 1$, the function $V_{t,i}(x)$ is shown in Figure 8 (lower plot), where $V_{t,i}(x) = 0$ as $x \leq r_t - r_a = 30$ and $V_{t,i}(x)$ is increased sharply as $x \rightarrow 40$ from $x = 30$. The function $V_{t,i}$ has the following properties:

(i) $\partial V_{t,i} / \partial \|\tilde{\xi}_{t,i}\| \geq 0$ as $V_{t,i}$ is a nondecreasing function with respect to $\|\tilde{\xi}_{t,i}\|$;

(ii) if $r_t - \|\tilde{\xi}_{t,i}\| \geq r_a$, namely the edges of the virtual tube are out of the avoidance area of the i th UAV, then $\sigma_t(r_t - \|\tilde{\xi}_{t,i}\|) = 0$; consequently, $V_{t,i} = 0$ and $\partial V_{t,i} / \partial \|\tilde{\xi}_{t,i}\| = 0$;

(iii) if $r_t - \|\tilde{\xi}_{t,i}\| < r_s$, namely one edge of the virtual tube has entered into the safety area of the i th UAV, then

$$\sigma_{t,i} (r_t - \|\tilde{\xi}_{t,i}\|) = 1$$

and there exists a sufficiently small $\epsilon_s > 0$ such that

$$s \left(\frac{r_t - r_s}{\|\tilde{\xi}_{t,i}\| + \epsilon_t}, \epsilon_s \right) \approx \frac{r_t - r_s}{\|\tilde{\xi}_{t,i}\| + \epsilon_t} < 1.$$

As a result,

$$V_{t,i} \approx \frac{k_3 (\|\tilde{\xi}_{t,i}\| + \epsilon_t)}{\epsilon_t (r_t - r_s)}$$

which will be very large if ϵ_t is very small.

The objective of the designed velocity command is to make $V_{t,i}$ be zero. This implies $r_t - \|\tilde{\xi}_{t,i}\| \geq r_a$ according to property (ii), namely the i th UAV will keep within the virtual tube.

B. Controller Design

The velocity command is designed as

$$\mathbf{v}_{c,i} = \mathbf{v}_{T,i} \quad (28)$$

$$\begin{aligned} \mathbf{v}_{T,i} = & -\text{sat} \left(\underbrace{\mathbf{A}_{t,23} \text{sat} (k_1 \tilde{\xi}_{l,i}, v_{m,i})}_{\text{Line Approaching}} + \underbrace{\sum_{j \in \mathcal{N}_{m,i}} -b_{ij} \tilde{\xi}_{m,ij}}_{\text{UAV Avoidance}} \right. \\ & \left. + \underbrace{c_i \mathbf{A}_{t,12} \tilde{\xi}_{t,i}}_{\text{Tunnel Keeping}}, v_{m,i} \right) \end{aligned} \quad (29)$$

with¹

$$b_{ij} = -\frac{\partial V_{m,ij}}{\partial \|\tilde{\xi}_{m,ij}\|} \frac{1}{\|\tilde{\xi}_{m,ij}\|} \quad (30)$$

$$c_i = \frac{\partial V_{t,i}}{\partial \|\tilde{\xi}_{t,i}\|} \frac{1}{\|\tilde{\xi}_{t,i}\|}. \quad (31)$$

This is a distributed control form. Unlike the formation control, neighboring UAVs' IDs of a UAV are not required. By active detection devices such as cameras or radars may only detect neighboring UAVs' position and velocity but no IDs, because these UAVs may look alike. This implies that the proposed distributed control can work autonomously without communication.

Remark 3. It is noticed that the velocity command (29) is saturated, whose norm will not exceed $v_{m,i}$. If the case such as $\|\tilde{\xi}_{m,ij}\| < 2r_s$ happens in practice due to unpredictable uncertainties out of the assumptions we make, this may not imply that the i th UAV has collided the j th UAV physically. In this case, the velocity command (28) degenerates to be

$$\begin{aligned} \mathbf{v}_{c,i} = & -\text{sat} \left(\mathbf{A}_{23} \text{sat} (k_1 \tilde{\xi}_{l,i}, v_{m,i}) - \sum_{j=1, j \neq i, j_i}^M b_{ij} \tilde{\xi}_{m,ij} \right. \\ & \left. + c_i \mathbf{A}_{t,12} \tilde{\xi}_{t,i} - b_{ij_i} \tilde{\xi}_{m,ij_i}, v_{m,i} \right) \end{aligned}$$

with $b_{ij_i} \approx \frac{k_2}{\epsilon_m \|\tilde{\xi}_{m,ij_i}\|^3}$. Since ϵ_m is chosen to be sufficiently small, the term $b_{ij_i} \tilde{\xi}_{m,ij_i}$ will dominate² so that the velocity command $\mathbf{v}_{c,i}$ becomes

$$\mathbf{v}_{c,i} \approx \text{sat} \left(\frac{k_2}{\epsilon_m} \frac{1}{\|\tilde{\xi}_{m,ij_i}\|^2} \frac{\tilde{\xi}_{m,ij_i}}{\|\tilde{\xi}_{m,ij_i}\|}, v_{m,i} \right).$$

This implies that, by recalling (13), $\|\tilde{\xi}_{m,ij_i}\|$ will be increased very fast so that the i th UAV can keep away from the j_i th UAV immediately.

Remark 4. In practice, the case such as $r_h - \|\tilde{\xi}_{h,i}\| < r_s$ may still happen in practice due to unpredictable uncertainties out of the assumptions we make. In this case, since ϵ_t is chosen to be sufficiently small, the velocity command $\mathbf{v}_{c,i}$ becomes

$$\mathbf{v}_{c,i} \approx \text{sat} \left(-\frac{k_3}{\epsilon_t (r_t - r_s)} \frac{\mathbf{A}_{t,12} \tilde{\xi}_{t,i}}{\|\tilde{\xi}_{t,i}\|}, v_{m,i} \right).$$

¹ $b_{ij} \geq 0$ according to the property (i) of $V_{m,ij}$; $c_i \geq 0$ according to the property (i) of $V_{t,i}$.

²Furthermore, we assume that the i th UAV does not conflict with others except for the j_i th UAV, or not very close to the edges of the virtual tube.

This implies that, by recalling (14), $\|\mathbf{A}_{t,12}\tilde{\xi}_{t,i}\|$ will be decreased so that the i th UAV can return back to the virtual tube immediately.

C. Stability Analysis

In order to investigate the basic virtual tube passing problem, a function is defined as follows

$$V = \sum_{i=1}^M \left(V_{1,i} + \frac{1}{2} \sum_{j=1, j \neq i}^M V_{m,ij} + V_{t,i} \right).$$

The derivative of V along the solution to (12),(13),(14) is

$$\begin{aligned} \dot{V} &= \sum_{i=1}^M \left(\text{sat} \left(k_1 \tilde{\xi}_{1,i}, v_{m,i} \right)^T \mathbf{A}_{t,23} \mathbf{v}_{c,i} \right. \\ &\quad \left. - \frac{1}{2} \sum_{j=1, j \neq i}^M b_{ij} \tilde{\xi}_{m,ij}^T (\mathbf{v}_{c,i} - \mathbf{v}_{c,j}) + c_i \tilde{\xi}_{t,i}^T \mathbf{A}_{t,12} \mathbf{v}_{c,i} \right) \\ &= \sum_{i=1}^M \left(\mathbf{A}_{t,23} \text{sat} \left(k_1 \tilde{\xi}_{1,i}, v_{m,i} \right) - \sum_{j=1, j \neq i}^M b_{ij} \tilde{\xi}_{m,ij} \right. \\ &\quad \left. + c_i \mathbf{A}_{t,12} \tilde{\xi}_{t,i} \right)^T \mathbf{v}_{c,i}. \end{aligned}$$

Since

$$\sum_{j=1, j \neq i}^M b_{ij} \tilde{\xi}_{m,ij} = \sum_{j \in \mathcal{N}_{m,i}} b_{ij} \tilde{\xi}_{m,ij}$$

by using the velocity input (28), \dot{V} becomes

$$\dot{V} \leq 0. \quad (32)$$

Before introducing the main result, two lemmas are needed.

Lemma 2. Under *Assumptions 1-4*, suppose that the velocity command is designed as (28). Then there exist sufficiently small $\epsilon_m, \epsilon_s > 0$ in b_{ij} and $\epsilon_t > 0$ in c_i such that $\|\tilde{\xi}_{m,ij}(t)\| > 2r_s$, $\|\tilde{\xi}_{t,i}\| < r_t - r_s$, $t \in [0, \infty)$ for all $\mathbf{p}_i(0)$, $i = 1, \dots, M$.

Proof. See Appendix. \square

With *Lemmas 1-2* in hand, we can state the main result.

Theorem 1. Under *Assumptions 1-4*, suppose (i) the velocity command in the distributed form is designed as in (28); (ii) given $\epsilon_0 \in \mathbb{R}_+$, if (15) is satisfied, then $b_{ij} \equiv 0$ and $c_i \equiv 0$ (this implies that the i th UAV is removed from the virtual tube mathematically). Then, for given $\epsilon_0 \in \mathbb{R}_+$, there exist sufficiently small $\epsilon_m, r_s \in \mathbb{R}_+$ in b_{ij} , $\epsilon_t \in \mathbb{R}_+$ in c_i and $t_1 \in \mathbb{R}_+$ such that all UAVs can satisfy (15) as $t \geq t_1$, meanwhile $\|\tilde{\xi}_{m,ij}(t)\| > 2r_s$, $\|\tilde{\xi}_{t,i}\| < r_t - r_s$, $t \in [0, \infty)$ for all $\mathbf{p}_i(0)$, $i = 1, \dots, M$.

Proof. According to *Lemma 2*, these VTOL UAVs are able to avoid conflict with each other and keep within the virtual tube, namely $\|\tilde{\xi}_{m,ij}(t)\| > 2r_s$, $\|\tilde{\mathbf{p}}_{t,i}\| < r_t$, $i \neq j$, $i, j = 1, 2, \dots, M$. In the following, the reason why the i th UAV is able to approach the finishing line $\overline{\mathbf{p}_{t,2}\mathbf{p}_{t,3}}$ is given.

The function V is not a Lyapunov function. The *invariant set theorem*[27, p. 69] is used to do the analysis.

- First, we will study the property of function V . Let $\Omega = \{\xi_1, \dots, \xi_M | V(\xi_1, \dots, \xi_M) \leq l\}$, $l > 0$. According to

Lemma 2, $V_{m,ij}$, $V_{t,i} > 0$. Therefore, $V(\xi_1, \dots, \xi_M) \leq l$ implies $\sum_{i=1}^M V_{1,i} \leq l$. Furthermore, according to *Lemma 1(iii)*, Ω is bounded. When $\|[\xi_1 \dots \xi_M]\| \rightarrow \infty$, then $\sum_{i=1}^M V_{1,i} \rightarrow \infty$ according to *Lemma 1(ii)*, namely $V \rightarrow \infty$. Therefore the function V satisfies the condition that the invariant set theorem is requires.

- Secondly, we will find the largest invariant set, then show all UAVs can pass the finishing line. Now, recalling the property (3), $\dot{V} = 0$ if and only if

$$\mathbf{A}_{t,23} \text{sat} \left(k_1 \tilde{\xi}_{1,i}, v_{m,i} \right) - \sum_{j=1, j \neq i}^M b_{ij} \tilde{\xi}_{m,ij} + c_i \mathbf{A}_{t,12} \tilde{\xi}_{t,i} = \mathbf{0} \quad (33)$$

where $i = 1, \dots, M$. Then $\mathbf{v}_{c,i} = \mathbf{0}$ according to (28). Consequently, by (1), the system cannot get “stuck” at an equilibrium value other than $\mathbf{v}_i = \mathbf{0}$. The equation (33) can be further written as

$$k_1 \kappa_{v_{m,i}} \mathbf{A}_{t,23} \tilde{\mathbf{p}}_{1,i} - \sum_{j=1, j \neq i}^M b_{ij} \tilde{\mathbf{p}}_{m,ij} + c_i \mathbf{A}_{t,12} \tilde{\mathbf{p}}_{t,i} = \mathbf{0}. \quad (34)$$

Let the 1st UAV be ahead, the closest to the finishing line $\overline{\mathbf{p}_{t,2}\mathbf{p}_{t,3}}$. Let us examine the following equation related to the 1st UAV that

$$k_1 \kappa_{v_{w,1}} \mathbf{A}_{t,23} \tilde{\mathbf{p}}_{1,1} - \sum_{j=2}^M b_{1j} \tilde{\mathbf{p}}_{m,1j} + c_1 \mathbf{A}_{t,12} \tilde{\mathbf{p}}_{t,1} = \mathbf{0}. \quad (35)$$

Since the 1st UAV is ahead, we have

$$(\mathbf{p}_{t,2} - \mathbf{p}_{t,1})^T \tilde{\mathbf{p}}_{m,1j} \geq 0 \quad (36)$$

where “=” hold if and only if the j th UAV is as ahead as the 1st one. On the other hand, one has

$$(\mathbf{p}_{t,2} - \mathbf{p}_{t,1})^T \mathbf{A}_{t,12} = 0. \quad (37)$$

Multiplying the term $(\mathbf{p}_{t,2} - \mathbf{p}_{t,1})^T$ at the left side of (35) results in

$$k_1 \kappa_{v_{w,1}} (\mathbf{p}_{t,2} - \mathbf{p}_{t,1})^T \mathbf{A}_{t,23} \tilde{\mathbf{p}}_{1,1} = (\mathbf{p}_{t,2} - \mathbf{p}_{t,1})^T \sum_{j=2}^M b_{1j} \tilde{\mathbf{p}}_{m,1j}$$

where (37) is used. Since $b_{1j} \geq 0$ and (36) holds for the 1st UAV, one has

$$(\mathbf{p}_{t,2} - \mathbf{p}_{t,1})^T \mathbf{A}_{t,23} \tilde{\mathbf{p}}_{1,1} \geq 0.$$

Since $(\mathbf{p}_{t,2} - \mathbf{p}_{t,1})^T \mathbf{A}_{t,23} \tilde{\mathbf{p}}_{1,1}(0) < 0$ according to *Assumption 2*, owing to the continuity, given $\epsilon_0 \in \mathbb{R}_+$, there must exist a time $t_{11} \in \mathbb{R}_+$ such that

$$\left(\frac{\mathbf{p}_{t,2} - \mathbf{p}_{t,1}}{\|\mathbf{p}_{t,2} - \mathbf{p}_{t,1}\|} \right)^T (\mathbf{p}_i(t) - \mathbf{p}_{t,2}) \geq -\epsilon_0$$

as $t \geq t_{11}$. At the time t_{11} , the 1st UAV is removed from (34) according to *Assumption 4*, namely it quits the virtual tube. The left problem is to consider the $M - 1$ UAVs, namely 2nd, 3rd, ..., M th UAVs. We can repeat the analysis above to conclude this proof. \square

V. CONTROLLER DESIGN FOR GENERAL VIRTUAL TUBE PASSING PROBLEM

So far, we have solved the basic virtual tube passing problem. Then, we are going to solve the general virtual tube passing problem. First, we define different areas for the whole airspace. Then, the general virtual tube passing problem is decomposed into several basic virtual tube passing problems. As a result, for UAVs in different areas, they have different controllers, like (28). Combining them together, the final controller is obtained.

A. Area Definition

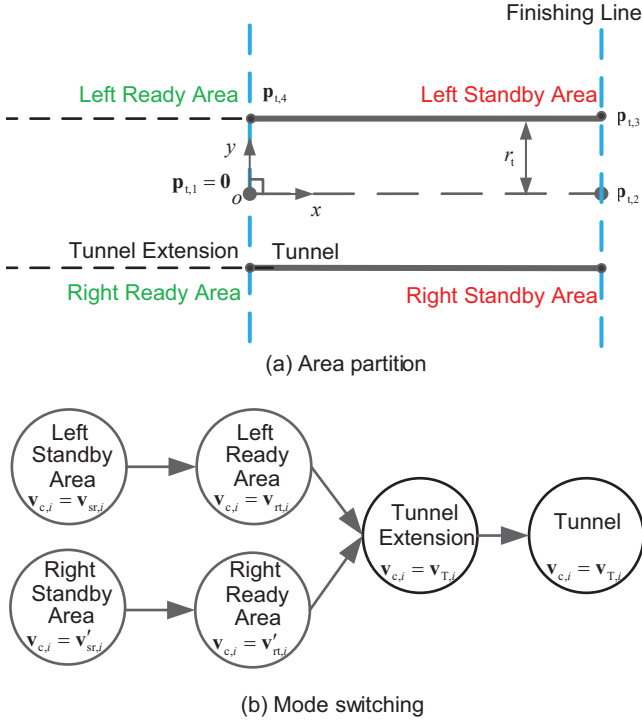


Fig. 9. Area definition and flight sequence.

As shown in Figure 9(a), the whole airspace is divided into six areas, namely *Left Standby Area*, *Left Ready Area*, *Right Standby Area*, *Right Ready Area*, *virtual tube*, and *virtual tube Extension*. Moreover, the Earth-fixed coordinate frame is built. For simplicity, let $\mathbf{p}_{t,1} = \mathbf{0}$ with x -axis pointing to $\mathbf{p}_{t,2}$ and y -axis pointing to its left side.

- *Left Standby Area* and *Right Standby Area* are the areas on the outside of *virtual tube* and the right side of *Starting Line* $\overline{\mathbf{p}_{t,1}\mathbf{p}_{t,4}}$, where $\mathbf{p}_{t,4} = [0 \ r_t]^T$. Concretely, if

$$\xi_i(1) > 0, \xi_i(2) > r_t$$

then ξ_i is in *Left Standby Area*. If

$$\xi_i(1) > 0, \xi_i(2) < -r_t$$

then ξ_i is in *Right Standby Area*.

- *Left Ready Area* and *Right Ready Area* are the areas on the outside of *virtual tube Extension* and the left side of *Starting Line* $\overline{\mathbf{p}_{t,1}\mathbf{p}_{t,4}}$. Concretely, if

$$\xi_i(1) \leq 0, \xi_i(2) > r_t$$

then ξ_i is in *Left Standby Area*. If

$$\xi_i(1) \leq 0, \xi_i(2) < -r_t$$

then ξ_i is in *Right Standby Area*.

- *virtual tube* and *virtual tube Extension* are a band. Concretely, if

$$\begin{aligned} \xi_i(1) &\leq 0 \ \& \ \xi_i(1) > \|\mathbf{p}_{t,1} - \mathbf{p}_{t,2}\| \\ -r_t &\leq \xi_i(2) \leq r_t \end{aligned}$$

then ξ_i is in *virtual tube Extension*. If

$$\begin{aligned} 0 &< \xi_i(1) \leq \|\mathbf{p}_{t,1} - \mathbf{p}_{t,2}\| \\ -r_t &\leq \xi_i(2) \leq r_t \end{aligned}$$

then ξ_i is in *virtual tube*.

B. virtual tube Passing Scheme and Requirements

As Assumption 2' points, at the beginning, UAVs may locate in the six areas. A flight sequence is given shown in Figure 9(b). The requirement is as follows.

- From *Left/Right Standby Area* to *Left/Right Ready Area*. UAVs are required to fly into *Left/Right Ready Area*, meanwhile avoiding conflict with other UAVs and keeping away from *virtual tube* and *virtual tube Extension*.
- From *Left/Right Ready Area* to *virtual tube Extension*. UAVs are required to fly into *virtual tube Extension*, meanwhile avoiding conflict with other UAVs and keeping away from *virtual tube*.
- From *virtual tube* and *virtual tube Extension* to *Finishing Line* $\overline{\mathbf{p}_{t,2}\mathbf{p}_{t,3}}$. UAVs are required to pass the *virtual tube* until it arrives near the finishing line $\overline{\mathbf{p}_{t,2}\mathbf{p}_{t,3}}$, meanwhile avoiding conflict other UAVs and keeping within the *virtual tube* and its extension.

C. Controller Design

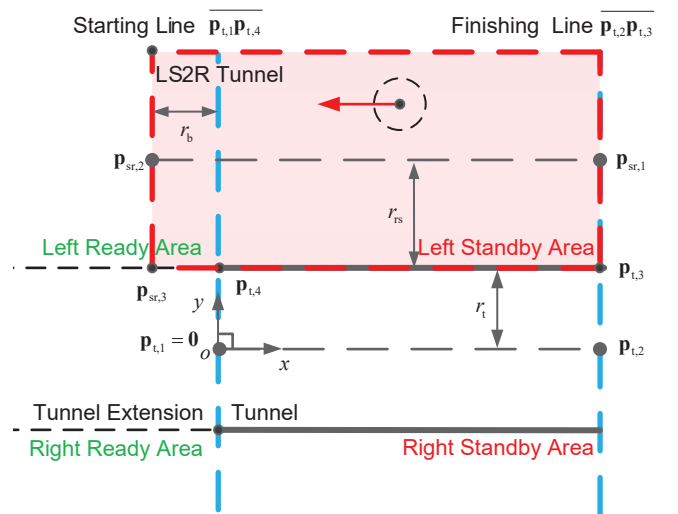


Fig. 10. LS2R virtual tube is designed for from Left Standby Area to Left Ready Area.

1) *From Standby Area to Ready Area*: As shown in Figure 10, a virtual virtual tube, named *LS2R virtual tube*, is designed

with the width $2r_{sr}$ and centerline starting from $\mathbf{p}_{sr,1} \in \mathbb{R}^2$ to $\mathbf{p}_{sr,2} \in \mathbb{R}^2$, where $r_{sr} > 0$ is often sufficiently large (10000 in the following simulation for example) that takes all UAVs in *Left Standby Area* in the virtual virtual tube. Moreover, we let all UAVs in *Left Standby Area* approach the finishing line $\overline{\mathbf{p}_{sr,2}\mathbf{p}_{sr,3}}$. Here

$$\mathbf{p}_{sr,1} = \begin{bmatrix} \mathbf{p}_{t,2}(1) \\ r_t + r_{sr} \end{bmatrix}, \mathbf{p}_{sr,2} = \begin{bmatrix} -r_b \\ r_t + r_{sr} \end{bmatrix}, \mathbf{p}_{sr,3} = \begin{bmatrix} -r_b \\ r_t \end{bmatrix}$$

where $r_b > 0$, $r_b = r_a$ for example. The intersection of *LS2R virtual tube* and *Left Ready Area* is a buffer with length r_b , which can make a UAV fly into *Left Ready Area* not only approaching it. According to (15), the controller is designed as $\mathbf{v}_{c,i} = \mathbf{v}_{sr,i}$, where

$$\mathbf{v}_{sr,i} = \text{sat}(\mathbf{v}_{1,i}(k_1, \mathbf{p}_{sr,2}, \mathbf{p}_{sr,3}) + \mathbf{v}_{m,i}(k_2) + \mathbf{v}_{t,i}(k_3, r_{sr}, \mathbf{p}_{sr,1}, \mathbf{p}_{sr,2}), v_{m,i}) \quad (38)$$

where

$$\mathbf{v}_{1,i}(k_1, \mathbf{p}_{t,2}, \mathbf{p}_{t,3}) \triangleq -\mathbf{A}_{t,23}(\mathbf{p}_{t,2}, \mathbf{p}_{t,3}) \text{sat}(k_1 \tilde{\xi}_{1,i}, v_{m,i}) \quad (39)$$

$$\mathbf{v}_{m,i}(k_2) \triangleq \sum_{j \in \mathcal{N}_{m,i}} b_{ij}(k_2) \tilde{\xi}_{m,ij} \quad (40)$$

$$\mathbf{v}_{t,i}(k_3, r_t, \mathbf{p}_{t,1}, \mathbf{p}_{t,2}) \triangleq -c_i(k_3, r_t) \mathbf{A}_{t,12}(\mathbf{p}_{t,1}, \mathbf{p}_{t,2}) \tilde{\xi}_{t,i}. \quad (41)$$

Furthermore, according to *Theorem 1*, UAVs in *Left Standby Area* will fly into *Left Ready Area*, meaning while avoiding colliding other UAVs and keeping within *LS2R virtual tube*, namely keeping away from *virtual tube* and *virtual tube Extension*.

Similarly, the controller for from *Right Standby Area* to *Right Ready Area* is designed as $\mathbf{v}_{c,i} = \mathbf{v}'_{sr,i}$, where

$$\mathbf{v}'_{sr,i} = \text{sat}(\mathbf{v}_{1,i}(k_1, \mathbf{p}'_{sr,2}, \mathbf{p}'_{sr,3}) + \mathbf{v}_{m,i}(k_2) + \mathbf{v}_{t,i}(k_3, r_{sr}, \mathbf{p}'_{sr,1}, \mathbf{p}'_{sr,2}), v_{m,i}) \quad (42)$$

with

$$\mathbf{p}'_{sr,1} = \begin{bmatrix} \mathbf{p}_{t,2}(1) \\ -r_t - r_{sr} \end{bmatrix}, \mathbf{p}'_{sr,2} = \begin{bmatrix} -r_b \\ -r_t - r_{sr} \end{bmatrix}, \\ \mathbf{p}'_{sr,3} = \begin{bmatrix} -r_b \\ -r_t \end{bmatrix}.$$

2) *From Ready Area to virtual tube Extension*: As shown in Figure 11, a virtual virtual tube, named *LR2T virtual tube*, is designed with the width $2r_{rt}$ and centerline starting from $\mathbf{p}_{rt,1} \in \mathbb{R}^2$ to $\mathbf{p}_{rt,2} \in \mathbb{R}^2$, where $r_{rt} > 0$ is sufficiently large that takes all UAVs in *Left Ready Area* in the virtual virtual tube. Moreover, all UAVs in *Left Ready Area* approach the finishing line $\overline{\mathbf{p}_{rt,2}\mathbf{p}_{rt,3}}$. Here

$$\mathbf{p}_{rt,1} = \begin{bmatrix} -r_{rt} \\ r_t + r_{rt} \end{bmatrix}, \mathbf{p}_{rt,2} = \begin{bmatrix} -r_{rt} \\ r_t - r_b \end{bmatrix}, \mathbf{p}_{rt,3} = \begin{bmatrix} 0 \\ r_t - r_b \end{bmatrix}.$$

The intersection of *LR2T virtual tube* and *virtual tube Extension* is a buffer with length r_b , which can make a UAV fly into

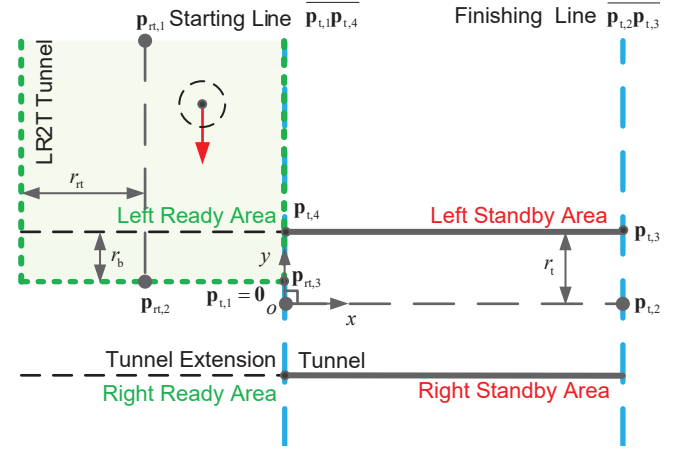


Fig. 11. LR2T virtual tube is designed for from Left Ready Area to virtual tube Extension.

virtual tube Extension not only approaching it. According to (15), the controller is designed as $\mathbf{v}_{c,i} = \mathbf{v}_{rt,i}$, where

$$\mathbf{v}_{rt,i} = \text{sat}(\mathbf{v}_{1,i}(k_1, \mathbf{p}_{rt,2}, \mathbf{p}_{rt,3}) + \mathbf{v}_{m,i}(k_2) + \mathbf{v}_{t,i}(k_3, r_{rt}, \mathbf{p}_{rt,1}, \mathbf{p}_{rt,2}), v_{m,i}) \quad (43)$$

According to *Theorem 1*, UAVs in *Left Ready Area* will fly into *virtual tube Extension*, meanwhile avoiding conflict with other UAVs and keeping within *LR2T virtual tube*, namely keeping away from *virtual tube*. Similarly, the controller for *Right Ready Area* to *virtual tube Extension* is designed as $\mathbf{v}_{c,i} = \mathbf{v}_{rt,i}$, where

$$\mathbf{v}'_{rt,i} = \text{sat}(\mathbf{v}_{1,i}(k_1, \mathbf{p}'_{rt,2}, \mathbf{p}'_{rt,3}) + \mathbf{v}_{m,i}(k_2) + \mathbf{v}_{t,i}(k_3, r_{rt}, \mathbf{p}'_{rt,1}, \mathbf{p}'_{rt,2}), v_{m,i}) \quad (44)$$

with

$$\mathbf{p}'_{rt,1} = \begin{bmatrix} -r_{rt} \\ -r_t - r_{rt} \end{bmatrix}, \mathbf{p}'_{rt,2} = \begin{bmatrix} -r_{rt} \\ -r_t - r_b \end{bmatrix}, \mathbf{p}'_{rt,3} = \begin{bmatrix} 0 \\ -r_t + r_b \end{bmatrix}.$$

3) *Final Controller*: With the design above, the final controller is designed as

$$\mathbf{v}_{c,i} = \begin{cases} \mathbf{v}_{T,i} (29) & \text{if } \xi_i \text{ in Tunnel and Tunnel Extension} \\ \mathbf{v}_{sr,i} (38) & \text{if } \xi_i \text{ in Left Standby Area} \\ \mathbf{v}'_{sr,i} (42) & \text{if } \xi_i \text{ in Right Standby Area} \\ \mathbf{v}_{rt,i} (43) & \text{if } \xi_i \text{ in Left Ready Area} \\ \mathbf{v}'_{rt,i} (44) & \text{if } \xi_i \text{ in Right Ready Area} \end{cases} \quad (45)$$

where $i = 1, 2, \dots, M$. Then, for given $\epsilon_0 \in \mathbb{R}_+$, there exist sufficiently small $\epsilon_m, r_s \in \mathbb{R}_+$ in b_{ij} , $\epsilon_t \in \mathbb{R}_+$ in c_i and $t_1 \in \mathbb{R}_+$ such that all UAVs can satisfy (15) as $t \geq t_1$, meanwhile $\|\tilde{\xi}_{m,ij}\| > 2r_s$ and $\|\tilde{\xi}_{t,i}\| < r_t - r_s$ when passing the virtual tube, $t \in [0, \infty)$ for all $\mathbf{p}_i(0)$, $i = 1, \dots, M$.

VI. SIMULATION AND EXPERIMENT

Simulations and experiments are given in the following to show the effectiveness of the proposed method, where a video about simulations and experiments is available on <https://youtu.be/LTNG7jWIBdY> or <http://weibo.ws/nJiiXJ>.

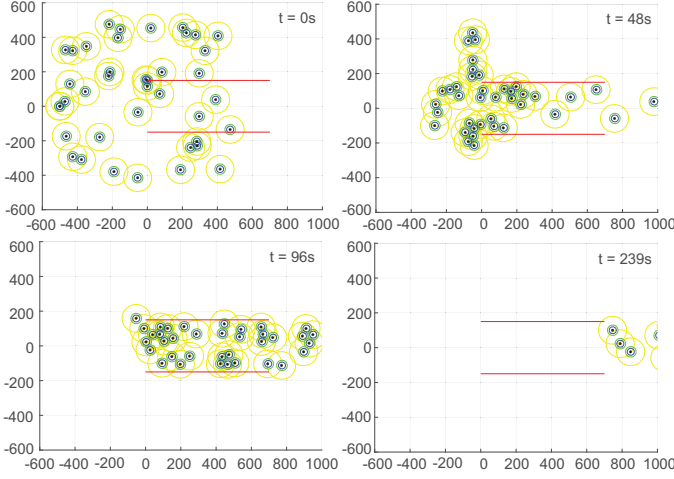


Fig. 12. UAVs' positions at different time.

A. Simulation

1) *Simulation with 40 UAVs*: We consider a scenario of $M = 40$ UAVs with $r_s = 20\text{m}$, $r_a = 30\text{m}$, $r_d = 80\text{m}$, $l_i = 5$ and $v_{m,i} = 5 + \frac{i}{4}\text{m/s}$, $i = 1, 2, \dots, M$. The virtual tube is a long horizontal band with the width $2r_t = 300\text{m}$ and centerline through $\mathbf{p}_{t,1} = [0 \ 0]^T\text{m}$ and $\mathbf{p}_{t,2} = [500 \ 0]^T\text{m}$. In order to show the effectiveness of the proposed method, the general virtual tube passing problem is considered directly. The initial positions of all UAVs are at everywhere with initial velocities being zero, shown by $t = 0\text{s}$ in Figure 12, where $\mathbf{p}_1(0) = [0 \ 149.9]^T\text{m}$ (the 1st UAV has a conflict with the virtual tube); $\mathbf{p}_2(0) = [-500 \ -0.1]^T\text{m}$ and $\mathbf{p}_3(0) = [-500 \ 0.1]^T\text{m}$ (the 2nd and 3rd UAVs have a conflict with each other initially) are set intentionally. The parameters of controller are $\epsilon_m = \epsilon_t = \epsilon_s = 10^{-6}$, $k_1 = k_2 = k_3 = 1$. With these conditions and parameters, the controller is performed for the simulation getting the results shown in Figure 12 and Figure 13. As shown in Figure 12, these UAVs enter into the virtual tube according to the sequence given in Figure 9(b), and pass the finishing line finally about $t = 239\text{s}$. As shown in Figure 13 (upper plot), during this process, the minimum distance of all pairs of UAVs is 0.2m because $\|\mathbf{p}_2(0) - \mathbf{p}_3(0)\| = 0.2\text{m}$. But, the minimum distance is increased rapidly and then always keeps above $2r_s = 40\text{m}$ (indicated by a dash line). This shows the effectiveness of the proposed controller that even if a UAV enters into the safety area of another UAV, it can keep away from the UAV rapidly. After this conflict, no conflict between any two UAVs will happen again. Similarly, as shown in Figure 13 (lower plot), during this process, the minimum distance from the virtual tube is 0.1m because of the 1st UAV being very close to the virtual tube. But, the minimum distance is increased rapidly and then always keeps above $r_s = 20\text{m}$ (indicated by a dash line). The reason can be found in Remark 4. After this conflict, no conflict with the virtual tube will happen again.

2) *Comparison of the Calculation Speed of Different Algorithms*: In order to show the advantage of the proposed algorithm, we compare the calculation speed with an optimization-based algorithm. In [16], a path-planning

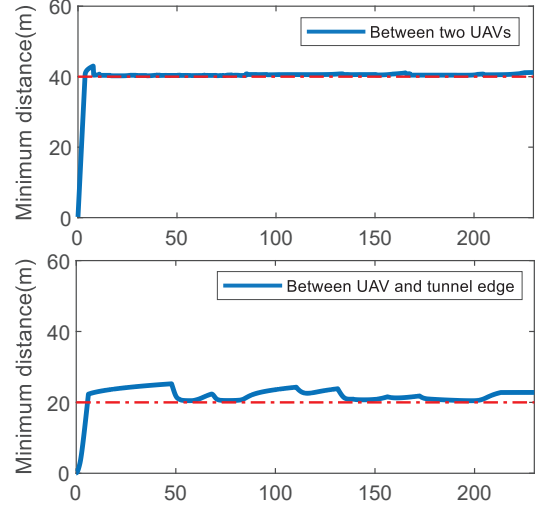


Fig. 13. Minimum distance among all UAVs and minimum distance from the virtual tube edge to all UAVs.

algorithm using Bezier curves with the open-source code at <https://github.com/byuflowlab/uav-path-optimization> is proposed, which can find the optimal solutions to the offline and online path-planning problem. We design a scenario that contains 10 UAVs with $r_s = 5\text{m}$, $r_a = 7.5\text{m}$, $r_d = 20\text{m}$, and a virtual tube with the width $2r_t = 200\text{m}$, centerline through $\mathbf{p}_{t,1} = [0 \ 0]^T\text{m}$ and $\mathbf{p}_{t,2} = [100 \ 0]^T\text{m}$. The initial position of 1st UAV $\mathbf{p}_1(0) = \mathbf{p}_{t,1} = [0 \ 0]^T$, while the other UAVs are distributed inside the virtual tube randomly with the same velocity $\mathbf{v}_i = [1 \ 0]^T\text{m/s}$, $i = 2, \dots, M$. For two different algorithms, we design 10 sets of random initial positions for the other UAVs, run the simulation on the same computer and record the *average calculation time* when the 1st UAV passes the finishing line of the virtual tube. Figure 14 shows the performance of the density on calculation speed by the changing the safety radius and the number of UAVs separately. As shown in Figure 14, for the same airspace, if the number of UAVs increases or the safety radius of UAVs gets larger, the calculation speed of optimization-based algorithm will decrease rapidly because the probability of constraint being triggered is increasing, which brings more complex calculations. On the contrary, the proposed controller can better deal with such situation, in other words, be suitable for dense and complex environment.

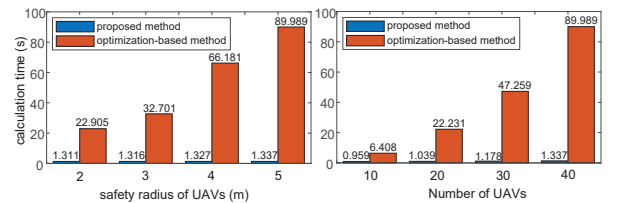


Fig. 14. The calculation speed of different algorithms.

B. Flight Experiments

As shown in Fig. 16, a set of experiments is carried out in a laboratory room with an OptiTrack motion capture system installed, which provides the positions and orientations of UAVs for distributed control. The laptop is connected to the Tello UAVs and OptiTrack by a local network, running the proposed controller and a real-time position plotting module.

In the first experiment, there are $M = 6$ UAVs to pass a virtual tube (indicated by a purple rectangle) as shown in Fig. 15. The virtual tube is a long horizontal band with the width $2r_t = 1.7\text{m}$ and centerline through $\mathbf{p}_{t,1} = [1.4 \ 0]^T\text{m}$ and $\mathbf{p}_{t,2} = [-1.4 \ 0]^T\text{m}$. Assuming that $r_s = 0.16\text{m}$, $r_a = 0.4\text{m}$, $v_{m,1} = v_{m,2} = 0.1\text{m/s}$ and $v_{m,i} = 0.2\text{m/s}$, $i = 3, 4, \dots, M$. The parameters of controller (45) are $\epsilon = r_s = 10^{-6}$, $k_1 = k_2 = k_3 = 1$ and $r_b = r_a$, $r_{sr} = r_{rt} = 10000\text{m}$. As shown in Fig 15(a), the initial positions of all UAVs (indicated by the dotted circle) are at everywhere with initial velocities being zero. We track UAVs from three perspectives: the main view, local view and the Graphical User Interface(GUI) view. As shown in Fig. 15(b), after take-off they all enter into the virtual tube according to the sequence given in Figure 9(b). By comparing with Fig. 15(c), we can get the result that the slower UAVs are gradually overtaken by the faster ones. Finally, as shown in Fig. 15(c), all UAVs complete their routes at 213.88 second, and they always keep a safe distance from others. This means each UAV passes the virtual tube and avoids each other successfully.

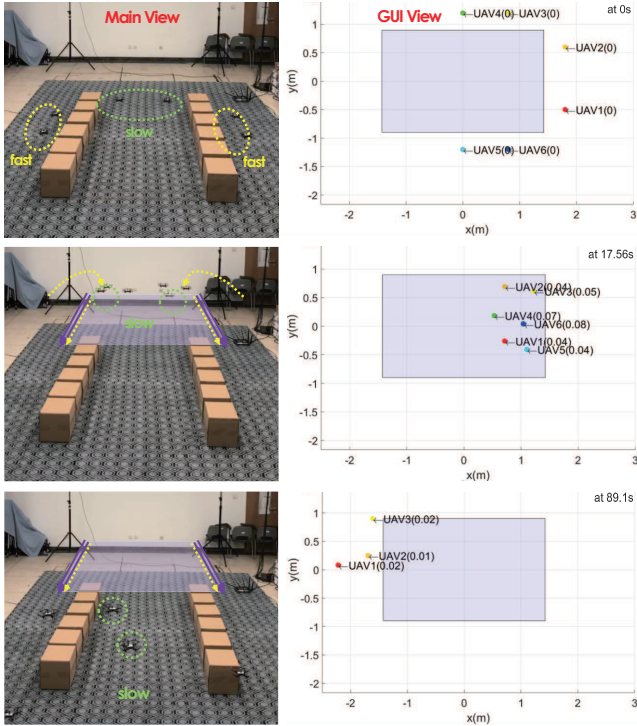


Fig. 15. The position, velocity and mode of each UAV during the first experiment

In the experiment, three virtual tubes are added into the flight progress as shown by $t = 0\text{s}$ in Figure 17. UAVs need to pass the three virtual tubes in order of clockwise rotation (indicated by the purple arrow), during which the

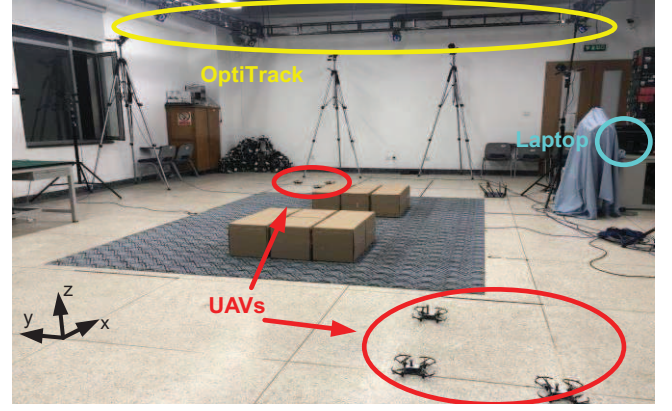


Fig. 16. Indoor experiment environment.

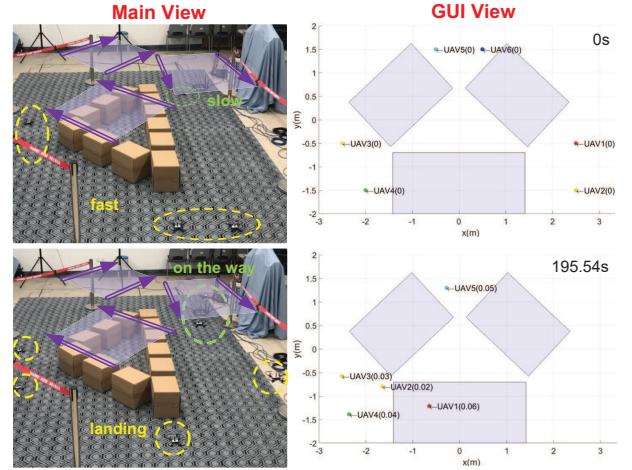


Fig. 17. Position and velocity during the experiment.

faster ones will overtake the slow ones. As shown in Figure 17 (lower plot), the faster UAVs pass the three virtual tube at 195.54 second, while the slower ones are still on the way. By comparing with Figure 17 (upper plot), we can observe that slow UAVs are overtaken by faster ones.

VII. CONCLUSIONS

The virtual tube passing problem, which includes passing a virtual tube, inter-agent conflict avoidance and keeping within the virtual tube, is studied in this paper. Based on the velocity control model of UAVs with control saturation, practical distributed control is proposed for multiple UAVs to pass a virtual tube. Every UAV has the same and simple control protocol. Lyapunov-like functions are designed elaborately, and formal analysis and proofs are made to show that the virtual tube passing problem can be solved, namely passing the virtual tube without getting trapped, avoiding conflict and keeping within the virtual tube. Besides the functional requirement, the safety requirement is also satisfied. By the proposed distributed control, a UAV can keep away from another one or return back to the virtual tube as soon as possible, once it enters into the safety area of another UAV or has a conflict with the virtual tube accidentally during it is passing the virtual tube. This is very necessary to guarantee the

flight safety. Simulations and experiments are given to show the advantages of the proposed method over other algorithms in terms of calculation speed of finding feasible solutions, and the effectiveness of the proposed method from the functional requirement and the safety requirement.

VIII. APPENDIX

A. Proof of Proposition 1

Proof. According to (1), we have

$$\mathbf{v}_i^T \dot{\mathbf{v}}_i = -l_i (\mathbf{v}_i^T \mathbf{v}_i - \mathbf{v}_i^T \mathbf{v}_{c,i}).$$

Then

$$\frac{d \|\mathbf{v}_i\|}{dt} = -l_i \|\mathbf{v}_i\| + \frac{1}{\|\mathbf{v}_i\|} \mathbf{v}_i^T \mathbf{v}_{c,i}$$

whose solution is

$$\begin{aligned} \|\mathbf{v}_i(t)\| &= e^{-l_i t} \|\mathbf{v}_i(0)\| + \int_0^t e^{-l_i(t-\tau)} \frac{1}{\|\mathbf{v}_i(\tau)\|} \mathbf{v}_i^T \mathbf{v}_{c,i}(\tau) d\tau \\ &\leq e^{-l_i t} \|\mathbf{v}_i(0)\| + \int_0^t e^{-l_i(t-\tau)} v_{m,i} d\tau. \end{aligned}$$

If $\|\mathbf{v}_i(0)\| \leq v_{m,i}$, then

$$\|\mathbf{v}_i(t)\| \leq v_{m,i}.$$

With the result, one has

$$\begin{aligned} \|\xi_i(t) - \xi_j(t)\| &\leq \|\mathbf{p}_i(t) - \mathbf{p}_j(t)\| + \left\| \frac{1}{l_i} \mathbf{v}_i \right\| + \left\| \frac{1}{l_j} \mathbf{v}_j \right\| \\ &\leq \|\mathbf{p}_i(t) - \mathbf{p}_j(t)\| + 2r_v. \end{aligned}$$

Since $\|\xi_i(t) - \xi_j(t)\| \geq r + 2r_v$, one further has

$$\|\mathbf{p}_i(t) - \mathbf{p}_j(t)\| + r_v > r + r_v.$$

Then $\|\mathbf{p}_i(t) - \mathbf{p}_j(t)\| > r$.

B. Proof of Lemma 2

The reason why these VTOL UAVs are able to avoid conflict with each other, which will be proved by contradiction. Without loss of generality, assume that $\|\tilde{\xi}_{m,i j_1}(t_0)\| = 2r_s$ occurs at $t_0 > 0$ first, i.e., a conflict between the i th UAV and the j_1 th UAV happening. Then, $\|\tilde{\xi}_{m,i j}(t_0)\| > 2r_s$ for $j \neq j_1$. Consequently, $V_{m,i j}(t_0) \geq 0$ if $j \neq j_1$. Since $V(0) > 0$ and $\dot{V}(t) \leq 0$, the function V satisfies $V(t_0) \leq V(0)$, $t \in [0, \infty)$. By the definition of V , we have

$$V_{m,i j_1}(t_0) \leq V(0).$$

According to (23), given any $\epsilon_{rs} > 0$, there exists a $\epsilon_s > 0$, such that

$$s(1, \epsilon_s) = 1 - \epsilon_{rs}.$$

Then, at time t_0 , the denominator of $V_{m,i j_1}$ defined in (26) is

$$\begin{aligned} (1 + \epsilon_m) \left\| \tilde{\xi}_{m,i j_1}(t_0) \right\| - 2r_s s \left(\frac{\left\| \tilde{\xi}_{m,i j_1}(t_0) \right\|}{2r_s}, \epsilon_s \right) \\ = 2r_s (1 + \epsilon_m) - 2r_s (1 - \epsilon_{rs}) \\ = 2r_s (\epsilon_m + \epsilon_{rs}) \end{aligned} \quad (46)$$

where $\epsilon_{rs} > 0$ can be sufficiently small if ϵ_s is sufficiently small according to (23). According to the definition in (26), we have

$$\frac{1}{2r_s (\epsilon_m + \epsilon_{rs})} = \frac{V_{m,i j_1}(t_0)}{k_2} \leq \frac{V(0)}{k_2} \quad (47)$$

where $\sigma_m \left(\left\| \tilde{\xi}_{m,i j_1} \right\| \right) = 1$ is used. Consequently, $V(0)$ is *unbounded* as $\epsilon_m \rightarrow 0$ and $\epsilon_{rs} \rightarrow 0$. On the other hand, for any j , we have $\left\| \tilde{\xi}_{m,i j}(0) \right\| > 2r_s$ by *Assumption 3*. Let $\left\| \tilde{\xi}_{m,i j}(0) \right\| = 2r_s + \epsilon_{m,i j}$, $\epsilon_{m,i j} > 0$. Then, at time $t = 0$, the denominator of $V_{m,i j}$ defined in (26) is

$$\begin{aligned} (1 + \epsilon_m) \left\| \tilde{\xi}_{m,i j}(0) \right\| - 2r_s s \left(\frac{\left\| \tilde{\xi}_{m,i j}(0) \right\|}{2r_s}, \epsilon_s \right) \\ \geq (1 + \epsilon_m) (2r_s + \epsilon_{m,i j}) - 2r_s \bar{s} \left(\frac{\left\| \tilde{\xi}_{m,i j}(0) \right\|}{2r_s} \right) \\ = 2r_s \epsilon_m + (1 + \epsilon_m) \epsilon_{m,i j}. \end{aligned}$$

Then

$$V_{m,i j}(0) \leq \frac{k_2}{2r_s \epsilon_m + (1 + \epsilon_m) \epsilon_{m,i j}}.$$

Consequently, $V_{m,i j}(0)$ is still bounded as $\epsilon_m \rightarrow 0$ no matter what ϵ_{rs} is. According to the definition of $V(0)$, $V(0)$ is still *bounded* as $\epsilon_m \rightarrow 0$ and $\epsilon_{rs} \rightarrow 0$. This is a contradiction. Thus

$$\left\| \tilde{\xi}_{m,i j}(t) \right\| > 2r_s, i \neq j \quad (48)$$

for $i, j = 1, 2, \dots, N$, $t \in [0, \infty)$. Therefore, the UAV can avoid another UAV by the velocity command (28).

The reason why a UAV can stay within the virtual tube is similar to the above proof. It can be proved by contradiction as well. Without loss of generality, assume that $\left\| \tilde{\xi}_{t,i}(t'_0) \right\| = r_t - r_s$ occurs at $t'_1 > 0$, i.e., a conflict happening first, while $\left\| \tilde{\xi}_{m,i}(t'_0) \right\| > r_t - r_s$ for $i = 1, \dots, M$. Similar to the above proof, one can also get a contradiction.

REFERENCES

- [1] M. Gharibi, R. Boutaba, and S. L. Waslander, "Internet of drones," *IEEE Access*, vol. 4, pp. 1148-1162, 2016.
- [2] S. Devasia and A. Lee, "A scalable low-cost-UAV traffic network (uNet)," *Journal of Air Transportation*, vol. 24, pp. 74-83, 2016.
- [3] L. E. Parker, "Path planning and motion coordination in multiple mobile robot teams," in *Encyclopedia of Complexity and System Science*, pp. 5783-5800, 2009.
- [4] W. Ren and Y. Cao, "Overview of recent research in distributed multiagent coordination," in *Distributed Coordination of Multi-agent Networks*. London, U.K.: Springer-Verlag, pp. 23-41, 2011.
- [5] G. Antonelli, "Interconnected dynamic systems: An overview on distributed control," *IEEE Control Systems*, vol. 33, no. 1, pp. 78-88, Feb. 2013.
- [6] Z. Yan, N. Jouandeau, and A. A. Cherif, "A survey and analysis of multi-robot coordination," *International Journal of Advanced Robotic Systems*, vol. 10, no. 399, Dec. 2013.
- [7] M. Hoy, A. S. Matveev, and A. V. Savkin, "Algorithms for collision-free navigation of mobile robots in complex cluttered environments: a survey," *Robotica*, vol. 33, no. 3, pp. 463-497, 2015.
- [8] K. K. Oh, M. C. Park, and H. S. Ahn, "A survey of multi-agent formation control," *Automatica*, vol. 53, pp. 424-440, Mar. 2015.
- [9] S. J. Chung, A. A. Paranjape, P. Dames, S. Shen, and V. Kumar, "A survey on aerial swarm robotics," *IEEE Transactions on Robotics*, vol. 34, no. 4, pp. 837-855, 2018.

- [10] S. P. Hou, C. C. Cheah, and J. J. E. Slotine, "Dynamic region following formation control for a swarm of robots," in *2009 IEEE International Conference on Robotics and Automation*, pp. 1929-1934, May. 2009.
- [11] F. Chen, and W. Ren, "A connection between dynamic region-following formation control and distributed average tracking," *IEEE Transactions on Cybernetics*, vol. 48, no. 6, pp. 1760-1772, 2017.
- [12] R. Dutta, L. Sun, D. Pack, "A decentralized formation and network connectivity tracking controller for multiple unmanned systems", *IEEE Transactions on Control Systems Technology*, vol. 26, no. 6, pp. 2206-2213, 2018.
- [13] X. Wang, V. Yadav, S. N. Balakrishnan, "Cooperative UAV formation flying with obstacle/collision avoidance", *IEEE Transactions on Control Systems Technology*, vol. 15, no. 4, pp. 672-679, 2007.
- [14] H. Liu, T. Ma, F. L. Lewis, et al, "Robust formation trajectory tracking control for multiple quadrotors with communication delays", *IEEE Transactions on Control Systems Technology*, vol. 28, no. 6, 2019.
- [15] M. Turpin, N. Michael, and V. Kumar, "Capt: Concurrent assignment and planning of trajectories for multiple robots," *The International Journal of Robotics Research*, vol. 33, no. 1, pp. 98-112, 2014.
- [16] B. T. Ingersoll, J. K. Ingersoll, P. DeFranco, and A. Ning, "UAV path-planning using Bezier curves and a receding horizon approach," *AIAA Modeling and Simulation Technologies Conference*, pp. 3675, 2016.
- [17] D. V. Dimarogonas, and K. J. Kyriakopoulos, "Connectedness preserving distributed swarm aggregation for multiple kinematic robots," *IEEE Transactions on Robotics*, vol. 24, no. 5, pp. 1213-1223, 2008.
- [18] F. Liao, R. Teo, J. L. Wang, X. Dong, F. Lin, and K. Peng, "Distributed formation and reconfiguration control of VTOL UAVs", *IEEE Transactions on Control Systems Technology*, vol. 25, no. 1, pp. 270-277, 2017.
- [19] Y. Liu, J. M. Montenbruck, D. Zelazo, et al., "A distributed control approach to formation balancing and maneuvering of multiple multirotor UAVs," *IEEE Transactions on Robotics*, vol. 34, no. 4, pp. 870-882, 2018.
- [20] B. Zhu, H. H. T. Liu, Z. Li, "Robust distributed attitude synchronization of multiple three-DOF experimental helicopters," *Control Engineering Practice*, vol. 36, pp. 87-99, 2015.
- [21] L. Wang, A. D. Ames, and M. Egerstedt, "Safety barrier certificates for collisions-free multirobot systems," *IEEE Transactions on Robotics*, vol. 33, no. 3, pp. 661-674, 2017.
- [22] E. G. Hernandez-Martinez, E. Aranda-Bricaire, F. Alkhateeb, E. A. Maghayreh, and I. A. Doush, "Convergence and collision avoidance in formation control: A survey of the artificial potential functions approach," in *Multi-Agent Systems—Modeling Control Programming Simulations and Applications*, Princeton, NJ:InTech, pp. 103-126, 2011.
- [23] Q. Quan, *Introduction to Multicopter Design and Control Singapore*, Springer, Singapore, 2017.
- [24] D. Panagou, D. M. Stipanović, and P. G. Voulgaris, "Distributed coordination control for multi-robot networks using Lyapunov-like barrier functions," *IEEE Transactions on Automatic Control*, vol. 61, no. 3, pp. 617-632, 2016.
- [25] DJI, Hardware Introduction. [Online]. Available: <https://developer.dji.com/onboard-sdk/documentation/introduction/osdk-hard>
- [26] N. Dunford, and J. T. Schwartz, *Linear Operators Part I: General Theory*, Interscience, New York, 1958.
- [27] J. J. E. Slotine, and W. Li, *Applied Nonlinear Control*, Englewood Cliffs, NJ: Prentice Hall, 1991.
- [28] G. B. Thomas, M. D. Weir, and J. Hass, *Thomas' Calculus*, Addison-Wesley, 2005.
- [29] R. A. Horn, and C. R. Johnson, *Matrix Analysis*, Cambridge University Press, 2013.



Rao Fu is working toward the Ph.D. degree at the School of Automation Science and Electrical Engineering, Beihang University (formerly Beijing University of Aeronautics and Astronautics), Beijing, China. His main research interests include UAV traffic control and swarm.



Mengxin Li is working toward the M.S. degree at the School of Automation Science and Electrical Engineering, Beihang University (formerly Beijing University of Aeronautics and Astronautics), Beijing, China. Her main research interests include flight safety and control of multicopter.



Donghui Wei received the B.S. and Ph.D. degrees in Aircraft Design from Beihang University, Beijing, China, in 2009 and 2020, respectively. He has been a senior engineer in Science and Technology on Complex System Control and Intelligent Agent Cooperation Laboratory. His research interests include ultra-low altitude flight control and swarm flight control.



Yan Gao is working toward the Ph.D. degree at the School of Automation Science and Electrical Engineering, Beihang University (formerly Beijing University of Aeronautics and Astronautics), Beijing, China. His main research interests include UAVs swarm and quadcopter control.



Quan Quan received the B.S. and Ph.D. degrees in control science and engineering from Beihang University, Beijing, China, in 2004 and 2010, respectively. He has been an Associate Professor with Beihang University since 2013, where he is currently with the School of Automation Science and Electrical Engineering. His research interests include reliable flight control, vision-based navigation, repetitive learning control, and timedelay systems.



Kai-Yuan Cai received the B.S., M.S., and Ph.D. degrees in control science and engineering from Beihang University, Beijing, China, in 1984, 1987, and 1991, respectively. He has been a Full Professor at Beihang University since 1995. He is a Cheung Kong Scholar (Chair Professor), jointly appointed by the Ministry of Education of China and the Li Ka Shing Foundation of Hong Kong in 1999. His main research interests include software testing, software reliability, reliable flight control, and software cybernetics.